ABSTRACT

JAMES G. GARTLAND. Response of an Electronic Sensor to Binary Solvent Mixtures in a Simulated Charcoal Bed. (Under the Direction of DR. DAVID A. FRASER)

A study was performed which evaluated the ability of a charcoal bed breakthrough detector to be utilized under conditions where a binary mixture of solvents was passed through a bed. A Taguchi Gas Sensor (TGS 812) was used.

Acetone and toluene were tested in a simulated charcoal bed system both singly and in binary mixtures over a range of concentrations. TGS response to acetone was much greater than to toluene. In addition, acetone achieved the charcoal service life endpoint (ie. 10% of the challenge concentration) more quickly. Toluene concentrations at the 10% breakthrough times for the acetone were insufficient to appreciably affect sensor response. It would thus appear that this detector can be utilized for the detection of a mixture of acetone and toluene if the alarm signal on the detector is preset for acetone. Sensor sensitivities were much weaker than found in a previous study with the same sensor.

TABLE OF CONTENTS

ACKNOWLEDGEMENTS

I would like to thank Dr. David Fraser for his excellent guidance and support in the completion of this project.

I would like to thank Dr. John Dement and Dr. James Watson for serving on my committee.

I would particularly like to thank Capt. Gary Bratt for the use of his prototype breakthrough indicator and for the advice he provided to me.

I am grateful to Mary Ann Sciandra for her aid in typing this report.

I especially would like to thank my parents for both the moral and financial support that made my years in Chapel Hill possible. Special thanks goes to Donna Schmoyer for her patience, understanding and love during the final stages of this report preparation.

Most importantly, I would like to thank God for the many answered prayers that made this project possible.

I. INTRODUCTION

A. GENERAL

The need for purification of air contaminated by potentially hazardous solvent vapors and gases is a problem encountered both in industry and the laboratory setting. One of the primary methods of purification involves the employment of activated carbon filter beds in ventilation systems. Although often an effective measure, activated carbon use presents an interesting risk-benefit situation. This problem arises from the difficulty of determining the exact point where the carbon bed reaches the end of its service life, the breakthrough point. This point is reached when the downstream concentration is 10% of the concentration of contaminant challenging the carbon. When the beds are discarded before reaching this point, there is an obvious monetary loss from replacing them more often than needed. If too much time passes before replacement, there is the more serious problem of potential risk to workers or the environment from escape of hazardous levels of contaminant through the bed. Finding a good method for determining end of service life thus becomes very important.

Unfortunately, there are no intrinsic aspects of carbon beds that allow easy service life determination. The carbon does not change color as it becomes full of adsorbed contaminants. There is no change in airflow resistance as the bed becomes saturated. A gain in mass of

the bed can be correlated to some degree with the degree of saturation, but since moisture is also adsorbed, changes in relative humidity make even this parameter difficult to use consistently (44).

One method that has found some success in the past was the use of carbon tetrachloride (CCl_4) as a nondestructive tracer gas. While CCl_4 was released upstream, air samples could be removed downstream of the filter for gas chromatograph analysis, or test elements (smaller models of the carbon beds) could be placed downstream and removed at intervals to evaluate saturation (45). A recent update of this concept has been suggested which would place a panel of carbon cartridges in a 4 by 4 matrix downstream of the carbon bed. These 16 cartridges could be individually removed over a period of time and analyzed to give an approximation of saturation increase over time and thus an estimate of service life (44). Although these methods have some usefulness, it would be better to have a means of continuously monitoring the downstream concentration of contaminants in order to get maximum benefit out of a carbon filtration system. A gas sensor would be able to determine when significant levels of contaminant are breaking through the filter bed, thus signifying the need for replacement.

A short discussion of carbon adsorption theory is presented in Appendix A.

An ideal monitor for detecting service life would have to meet a number of performance characteristics. It should be small, rugged, inexpensive and be capable of continuous operation. It should actively indicate (usually by alarm) the presence of the preset contaminant level without outside intervention. It should respond reliably to contaminant gases and vapors over a range of several orders of

magnitude with a time resolution of a few minutes and be sensitive at the toxic limits of the contaminant (29,43).

B. SERVICE LIFE MONITORING METHODS

There is probably no monitor or sensor which meets all of the requirements discussed previously. A critical review of some of the techniques suggested for monitoring of breakthrough should allow a proper choice to be made for further evaluation.

1. Catalytic oxidation (12,27,29,42)

Gas detectors operating on the catalytic oxidation principle work by measuring the amount of heat liberated when an organic molecule reacts exothermically with an oxidant. Monitors based on this technique have relatively poor response, especially at low concentrations where they must be zeroed every few moments. They not only have poor response to halogenated hydrocarbons, but are easily poisoned by them. A relatively expensive amplifier circuit is required for this sensor.

2. Gas chromatography (12,27)

Systems based on gas chromatography analysis have some very positive qualities. They give highly accurate, continuous responses to most gases. Unfortunately, they are often too complicated for easy use and require extensive training of personnel for reliable results. Another major consideration is the high cost of such systems.

3. Nondispersive infrared (12,27,29)

These systems are based on the absorption of infrared radiation by contaminants. The instrumentation is relatively complex. A separate setting must usually be made for each contaminant and corrections must often be made for interference from other contaminants or water vapor. The instruments are also moderately expensive.

4. Ultraviolet (UV) ionization (27,29)

These systems rely on high energy UV radiation causing the ionization of molecules, which induces current flow between two electrodes. This technique is among the better ones suggested for breakthrough monitoring. Most of the commercially used hydrocarbons, including the chlorinated ones, can be detected by UV ionization systems. Monitors based on these techniques have the advantages of being light, safe and easy to use. As with infrared systems, detectors are moderately expensive.

5. Color-changing indicators (Detector tubes) (12,29,39)

This method relies on a change in color of a specific adsorbent when air containing a given contaminant is passed through it. The color change is usually the result of a reduction-oxidation reaction. The concept has been evaluated for respirator cartridge breakthrough (29,39).

A major disadvantage of detector tubes is the lack of continuous response. There are also problems occasionally with sensitivity and interferences. The technique still has usefulness for spot checks to obtain qualitative measures of breakthrough.

6. Piezoelectric microbalances (29,42)

This method works on the principle of a small amount of contaminant mass altering the vibrational frequency imposed on a quartz crystal by an applied electrical AC frequency in the range of 9 to 15 MHz. While these systems have the advantages of high sensitivity, small size and relatively simple electronics, there is a large problem with interferences. The sensor can react to water and even aerosols. Some degree of specificity can be arranged if a given contaminant is being sought, but this involves coating the crystal and the reactions with these coatings are usually nonreversible.

7. Flame ionization systems (27,29)

In these monitors, the air to be sampled flows through a hydrogen flame and the ions thus produced induce a flow of current proportional to the concentration of the contaminant to an electrode located adjacent to the flame. These systems are also among the better breakthrough monitors, especially since almost all hydrocarbons may be detected by them. High cost is again a disadvantage.

8. Metallic oxide semiconductor (MOS) sensors

Instruments based on the metallic oxide semiconductor sensor have shown some promise as breakthrough monitors. They were the sensor type chosen for further research in this paper and in several studies involving respirators (6,25), including a NIOSH (National Institute for Occupational Safety and Health) study on end-of-life monitors for respirators (29).

In the following section, a review of the metallic oxide

semiconductor literature is presented in order to gain a better understanding of the theory, mechanisms and uses of these sensors. In addition, a review of the literature is presented pertaining to the Taguchi Gas Sensor (TGS), which was chosen for further study in this paper.

C. REVIEW OF MOS SENSOR LITERATURE

1. Early history

It was noticed early in the history of semiconductor development that the presence of contaminant gases could alter the conductivity of the semiconductor. Among the first investigators to attempt to find a practical use for this phenomenon were Seiyama, et al, (41) in 1962. A thin film of zinc oxide was utilized as a gas detector in a gas chromatograph in the place of the thermal conductivity cell usually used. Using nitrogen as a carrier gas, this sensor was tested for response to toluene, benzene, ethyl ether, ethyl alcohol, propane and carbon dioxide and was found to be much more sensitive than the thermal conductivity cell.

Later work by Seiyama and Kagawa (40) involved testing of thin films of several semiconductor materials. When tested against hydrogen, carbon dioxide and ethanol, sensors composed of thin films of zinc oxide, cadmium oxide, ferric oxide and tin oxide showed better sensitivity than other metal oxides. It is interesting to note that, with zinc oxide, a linear relationship between detector response and contaminant concentration was only obtained after plotting on a log-log scale, thus suggesting a power relationship.

2. Band theory

To understand the response of the MOS sensor, one must first consider the sensor at the atomic level.

In order for the conductivity of the semiconductor to be altered by a gaseous contaminant, an adsorption reaction involving electron transfer (chemisorption) must occur (42). Oxides of transition and heavy metals such as tin are semiconductors because these metals can exist in different oxidation states. These oxides are non-stoichiometric. Tin oxide semiconductors are classified as n-type, having an excess of metal ions. A deficiency of metal ions occurs in a p-type semiconductor. Only n-type semiconductors will be discussed here unless otherwise noted. Electrostatic neutrality is maintained in n-type semiconductors by the excess metal occurring as ions of a lower charge than the parent metal ion, e.g. Sn^{2+} in SnO_2 (14). The energy levels of an n-type semiconductor are depicted in Figure 1. The two bands of allowed energy, the conduction and valence bands, are separated by a band gap, where only localized states can be occupied by electrons. These states include donor levels near the conduction band and trap levels near the valence band. At thermal equilibrium, the probability of occupation of these states is given by Fermi statistics and described by the Fermi level, as seen in Figure 1 (18).

3. Conductivity and chemisorption

The energy bands are altered as the surface of the semiconductor is approached. Electronic surface states may be caused by intrinsic defects of the semiconductor or by adsorption of other atoms or molecules. When the surface states accept a charge, an electrical

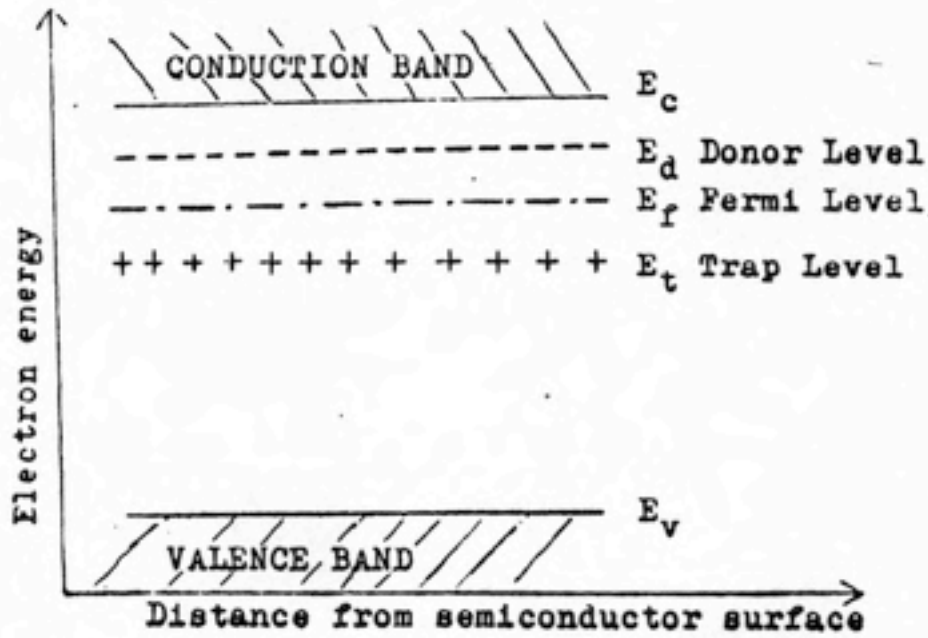

Figure 1. Generalized energy levels for n-type semiconductors

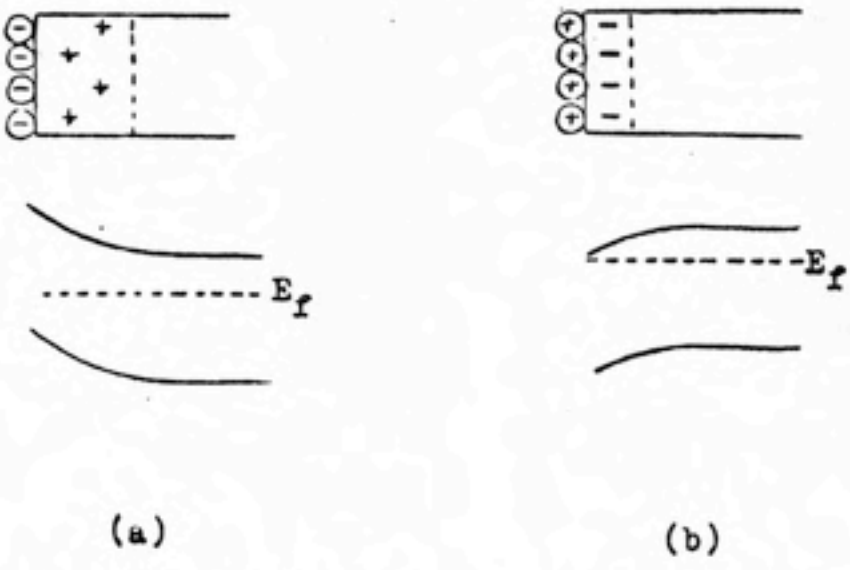

Figure 2. Chemisorption and space charge layer formation. a) Oxygen adsorption b) Reducing gas adsorption

double layer is formed of equal but opposite charge in a layer defined as the space charge layer (18).

The conductivity of the sensor can be maintained, decreased or increased, depending on which type of reaction occurs at its surface. Since physical adsorption does not involve an exchange of electrons, any contaminant reacting only by this method will not cause a conductivity change and will not be detected. Noble gases, which are physisorbed, are not detected by MOS sensors. It is the chemisorption reactions which lead to conductivity changes. These reactions are of two main types. The first is depletive chemisorption, in which electrons are extracted from the conduction band. The adsorption of oxygen in an ionic form, such as O_2^-, O^- or O^{2-}, on an n-type MOS involves depletive chemisorption (21). Oxygen adsorption thus causes a drop in conductivity, as electrons are pulled out of the conduction band of the MOS. This increases the negative charge at the surface and causes the formation of a positive space charge layer and bending of the conduction band away from the Fermi level as can be seen in Figure 2(a). This process continues until equilibrium is reached, where the electron capture rate of the adsorbate equals the rate of emission back to the conduction band of the semiconductor (26).

The other type of chemisorption reaction causes a conductivity increase. This occurs when a reducing gas is adsorbed in the presence of an ambient atmosphere containing oxygen. Exposure of the MOS to this ambient leads to the formation of a chemisorbed oxygen layer. The reducing gas reacts with the oxygen layer, leading to a donation of electrons into the conduction band. These donations cause an increase in conductivity of the MOS as electron density in the bulk of the

semiconductor is increased, ie. a negative space charge layer is formed (26). The conduction band is bent towards the Fermi level during this process, as can be seen in Figure 2(b). Since equilibrium is reached at a point dependent on the partial pressure of the reducing gas, the conductance of the sensor can be related to varying concentrations of reducing contaminants (28).

4. MOS response to reducing agents

Carbon monoxide (CO) can be adsorbed on a MOS surface in the form of the positively charged ion, CO^+. This reducing form of the gas reacts with the chemisorbed oxygen as described above with resultant desorption of carbon dioxide and the injection of the electrons released from the oxygen back into the bulk of the MOS. The resulting increase in conductivity reaches an equilibrium level as oxygen is re-adsorbed from the ambient atmosphere, thus relating conductivity to the partial pressure of CO (14).

Windischmann and Mark (51) investigated the adsorption of CO on a thin film of tin oxide (SnO_2). They designed their sensor to detect CO reproducibly in the 1 to 100 ppm range in the presence of an ambient atmosphere consisting of 10% oxygen, 3% water, 500 ppm sulfur dioxide, 150 ppm nitric oxide, 9% carbon dioxide and the balance, nitrogen. Within a temperature range of 200 to 500 °C, the sensor conductance (G) increases with increasing CO partial pressure (P_{CO}) according to the relation:

$$G = G_o + (K)(P_{CO})^{1/2} \qquad (1)$$

where G_o is the background conductance in the absence of CO and

K is a constant with respect to P_{CO}.

Stetter (42) investigated the adsorption of CO on cobalt oxide (Co_3O_4). This is a p-type semiconductor (deficiency of metal ions) as compared to the n-type SnO_2 (excess metal ions) studied by Windischmann and Mark (51). At a constant temperature, the conductivity (σ) and CO partial pressure (P_{CO}) followed the relation:

$$\ln(\sigma/\sigma_o) = \ln K + (m)(\ln P_{CO}) \qquad (2)$$

where σ_o is the background conductance, K is both a constant with respect to P_{CO} and the y-intercept of a log-log plot of σ/σ_o vs P_{CO} with m as the slope.

This shows a power relation between conductivity and CO partial pressure of the form:

$$\sigma/\sigma_o = (K)(\ln P_{CO})^m \qquad (3)$$

Seiyama and Kagawa (40) studied the response of a thin film of zinc oxide (ZnO) to a variety of organic compounds. It was found that the sensor sensitivity increased with the number of carbon atoms in normal chain compounds. Substituent effects of normal chain compounds having the same number of carbon atoms showed the following order of response sensitivity:

amine > ether > mercaptan > alcohol > ketone > aldehyde > carboxylic acid > nitrile.

It was noted that this is the same general order for electron donating properties of the functional groups. Greater sensitivity occurred in compounds with the most nucleophilic groups. This is to be expected in n-type MOS like ZnO and SnO_2 where the conduction band accepts the donated electrons readily. Response for aromatic compounds was more complex, but some correlation was found between dipole moment and sensitivity. This correlation of increasing polarization with

increasing sensitivity did not hold for aromatic halides.

5. Factors affecting MOS response

Any gas which can be adsorbed and react to cause electron transfer will cause a change in conductivity of a MOS. It is for this reason that consideration must be given to the combined effects of two or more components in a mixture. When a MOS is calibrated for detection of a specific compound, the interference of other compounds may fall into one of two categories. Proportional interference occurs when every X ppm of interference gas results in a response of Y ppm in terms of the gas of interest. In other words, 100 ppm of gas A could show a reading of 10 ppm of gas B when the MOS is calibrated for B. The other type of interference is known as tolerance interference. In a response of this type, the MOS will not respond to the interference gas A until a critical concentration is reached. After this critical concentration is reached, the MOS shows a large response to gas A in terms of gas B (24).

Temperature is found to have a major effect on sensor response. The adsorption of a gas on a given MOS is a temperature-dependent process. Different gases will have differing temperatures which will produce optimum response. Firth, et al, (14) found that the conductivity change produced by a gas at a given concentration usually increased as the temperature of the MOS increased, passing through a maximum and decreasing beyond a certain temperature. This optimum temperature will vary between gases in a chemical series, but the shapes of the curves will be similar (21). It is clear that by designing the circuit associated with the MOS so that operating

temperature can be varied, that a certain degree of specificity can be obtained.

Moisture is another factor affecting sensor response. Although the exact mechanism of this effect is not clear, Boyle and Jones (5) suggested that water is adsorbed with preferential alignment of the positive section of the dipole with the MOS surface. Electrons would then be pulled to the MOS surface to form a negative space charge layer and increase conductivity. Morrison (28) disagreed with this concept, stating that the reaction would be too endothermic. He suggested that the water changes the surface state energy of the oxygen through neutralization of surface electric fields which have charged areas attracting oxygen ions. More research is needed to clarify these mechanisms. It is clear that relative humidity, being a product of temperature and moisture, will have an effect on sensor response. The baseline conductivity of a MOS in an ambient atmosphere will increase with increasing relative humidity. This can cause problems, as most measurements utilizing MOS sensors have the ratio of contaminant to ambient response of the sensor as the factor related to concentration.

6. Techniques to control MOS sensor sensitivity

One of the most effective methods for controlling MOS sensor sensitivity is the use of dopants or chemical additives. Two mechanisms have been suggested for the actions of these dopants (52). The first is chemical interaction in which the dopant assists the redox process on the surface of a SnO_2 sensor. At the optimum temperature, a reactant will first adsorb on the dopant particles and then migrate to the SnO_2 surface to react with the adsorbed oxygen. This

increased adsorption leads to increased surface conductivity in the sensor and thus a stronger response to reducing gases. This interaction involves a change of oxidation state in the semiconductor and appears to occur in SnO_2 doped with platinum or palladium. The other suggested mechanism, electronic interaction, occurs when the dopant interacts with the semiconductor as an electron donor or acceptor. A change in the electronic state of the dopant due to reaction with a reducing gas will thus cause an accompanying change in the semiconductor surface conductivity. Electronic interactions involve a change in the oxidation state of the dopant as compared to the change in the state of the semiconductor which occurs with chemical interaction. Electronic interaction has been suggested as the mechanism for SnO_2 with silver as the dopant.

The proper choice of dopant can help to increase specificity of the sensor for given compounds or reduce interference from other compounds. Nitta and Haradome (33) found that utilizing thorium dioxide (ThO_2) as a dopant of a SnO_2 thick film semiconductor increased the specificity of the sensor for carbon monoxide (CO) over hydrogen (H_2) while also achieving a high degree of independence in the response of the sensor to humidity. In another study, Nitta, et al, (34) found that doping SnO_2 with Nb, V, Ti or Mo again gave increased freedom from relative humidity and temperature effects on sensor response. Jones (21) reported that uranium dioxide (UO_2) is relatively insensitive to most gases, but response is greatly increased when doped with Pt, Pd or Ga.

The physical form of the MOS can also affect sensitivity. Oyabu conducted studies on tin oxide with Pd as the dopant. In one study,

he used a thin film of SnO_2 (36) and the other a thick film (37). The thin film was formed by vapor deposition of SnO_2, while the thick film was deposited in the form of a thin paste. In both studies, the sensors were tested for response to ethanol, carbon monoxide, isobutane and hydrogen. The thin film sensor responded only to carbon monoxide and ethanol, while the thick film responded only to hydrogen and ethanol. Jones (21) investigated ZnO in the form of a single crystal, a polycrystalline mass and a highly sintered compressed disc. The disc and single crystal forms showed similar response to carbon monoxide, methane and water. The polycrystalline mass showed a much stronger response to methane at higher temperatures. It was suggested that there is a higher concentration of surface defects on these masses that would provide sites for greater adsorption of methane.

Pretreatment with heated gases and use of surface state additives are two more methods which have been found to affect MOS sensitivity. Lalauze and Pijolat (23) found that pretreatment by heating a SnO_2 sensor to 500 ^{o}C in a 1000 ppm sulfur dioxide-air mixture changed the normal SnO_2 maximum response temperature sufficiently that a relatively specific benzene detector could be developed. They suggested that a H_2S-specific detector could be developed using a similar technique. Morrison (28) investigated the use of surface state additives. This technique involved a literature search to find a contaminant-specific reagent. The reagent could then be coated on a MOS which would respond to electronic changes resulting from the reaction of the reagent. A NO_2-specific sensor was developed by coating nickel oxide with Saltzmann reagent, used in colorimetric tests. A xylene-specific sensor was developed by utilizing titanium dioxide coated with vanadium

pentoxide, a catalyst for oxidation of xylene. As in the discussion of piezoelectric balances earlier, the coating of the sensor often leads to irreversible responses in the sensors using this technique.

D. REVIEW OF TAGUCHI GAS SENSOR (TGS) LITERATURE

1. Introduction

The Taguchi Gas Sensor (TGS) was the MOS sensor chosen for further study in this project. The TGS meets a number of the requirements listed earlier for an ideal breakthrough monitor. It has the ability to detect a number of gases at low concentrations and with repeatable responses due to reversible reactions. The TGS is designed to fit some of the other requirements also. It is small, inexpensive, shock and vibration resistant and can be operated from a low voltage power supply (12,13). The TGS also suffers from the disadvantages associated with the MOS, in particular, the sensitivity to temperature and humidity changes (47).

A list of some of the contaminants detected by the TGS can be found in Appendix B.

The TGS was developed by N. Taguchi and has been marketed by Figaro Engineering since 1968. Over 13 million TGS sensors were in use worldwide as of August, 1981 (12). There are a number of TGS models, varying in design features such as dopants, which have increased selectivity for given groups of contaminants. The TGS 812 is the model designed for best response to toxic gases. The following discussions will concern the TGS 812 unless otherwise noted.

2. TGS 812 structure

The structure of the TGS 812 gas sensor can be seen in Figure 3. The TGS 812 is composed of a thin layer of sintered SnO_2 coated on a small ceramic cylinder (4 mm X 1 mm). A small coil of 60 micron diameter chrome alloy wire is located inside the cylinder to serve as a heater coil. It has a resistance of 38 ohms. Two 80 micron diameter gold alloy wires are deposited on the ceramic along with the SnO_2 to serve as electrodes, allowing measurement of resistance changes. The heater and electrode wires are spotwelded to pins arranged to fit a 7 pin miniature tube socket.

The sensor base and cover are composed of nylon 66 which has a deformation temperature in excess of 240 °C. The sensor case has upper and lower openings covered with a flameproof double layer of 100 mesh stainless steel gauze. Independent tests have confirmed that this mesh will prevent a spark produced inside the flameproof cover from igniting an explosive 2:1 mixture of hydrogen and oxygen. The TGS 812 also is tested mechanically with vibration and shock tests. The parameters for safe operation include a maximum power dissipation for the sensor of 15 MW, a maximum circuit voltage of 24 V and a heater voltage of 5.0 V $\pm$ 0.2 V (9,11).

3. TGS 812 mechanism of operation

The design of the TGS 812 gives it some advantages over other sensor types. The symmetrical geometry of the cylinder allows uniform temperature to be spread along the active semiconductor layer, while also reducing heating requirements because of a high surface-to-volume ratio (47). The sintering of the tin oxide powder deposited on the

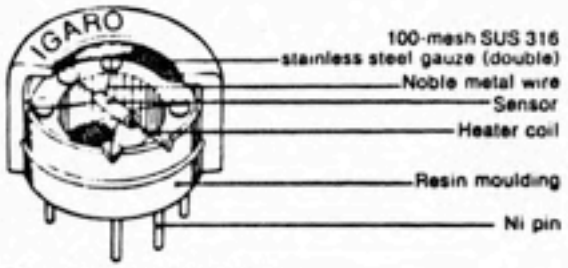

TGS 812 CONFIGURATION.

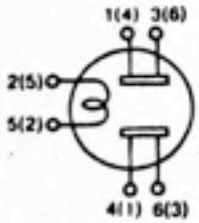

TGS 812 DIAGRAM OF THE ELECTRIC CIRCUIT.

◆Remarks:

Pins numbered 1 and 3 are connected internally.
Pins numbered 4 and 6 are connected internally.

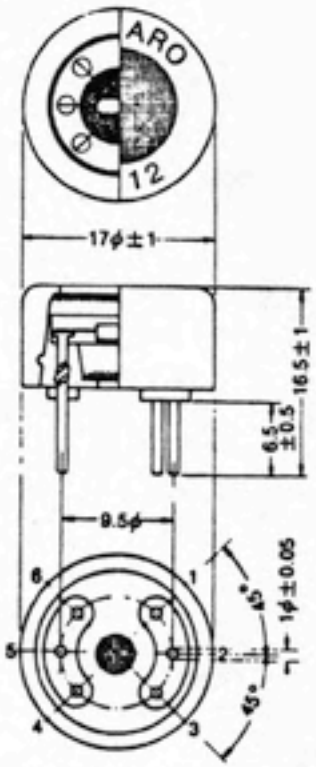

Dimensions in millimeter

TGS 812 STRUCTURAL SPECIFICATIONS.

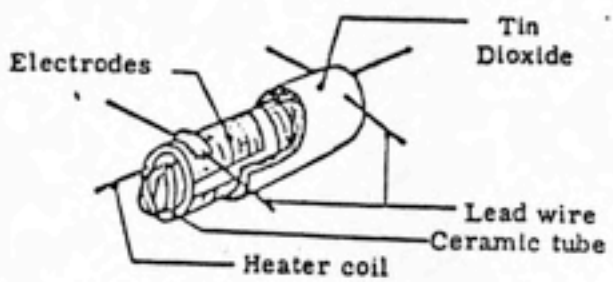

Configuration of gas sensor

Figure 3. Structural Diagrams of the TGS 812.

ceramic allows it to have a higher sensitivity, comparable with the sensitivity of thin film sensors. Morrison (28) suggested that the contact resistance between grains of the sintered powder was the dominant factor in overall TGS sensor resistance. With non-sintered grains, such as would be found in a compressed pellet, electrons flowing from one grain to another must first flow over a surface potential barrier, as in Fig. 4(a). Current between grains is very sensitive to the barrier. Sintering reduces this barrier by providing a "neck" or channel similar in thickness to thin film, ie, a few hundred angstroms. These channels are depicted in Fig. 4(b).

Adsorption of oxygen and reducing gases on these necks has similar effects to adsorption on thin films. Oxygen adsorption increases the barrier height by decreasing the width of the channel through which the current flows and increasing sensor resistance. The adsorption of reducing gases and reaction with the adsorbed oxygen decreases the barrier height and thus decreases the sensor resistance.

Clifford and Tuma (10) showed the electron transfer controlled by this potential barrier to be the rate limiting step in oxygen ionosorption on the TGS 812. They found the conductance (σ) of the sensor to be determined by the surface barrier potential (eV_s) at a given temperature (T) by the relation:

$$\sigma = \sigma_0 \exp[-eV_s/KT] \qquad (4)$$

and the barrier potential to be determined by the surface concentration of ionosorbed oxygen (N_t) by the Schottky relation:

$$V_s = e(N_t)^2/2K_s\varepsilon_0 N_d \qquad (5)$$

where N_t is the surface density of ionosorbed oxygen, $K_s\varepsilon_0$ is the semiconductor permittivity and N_d is the

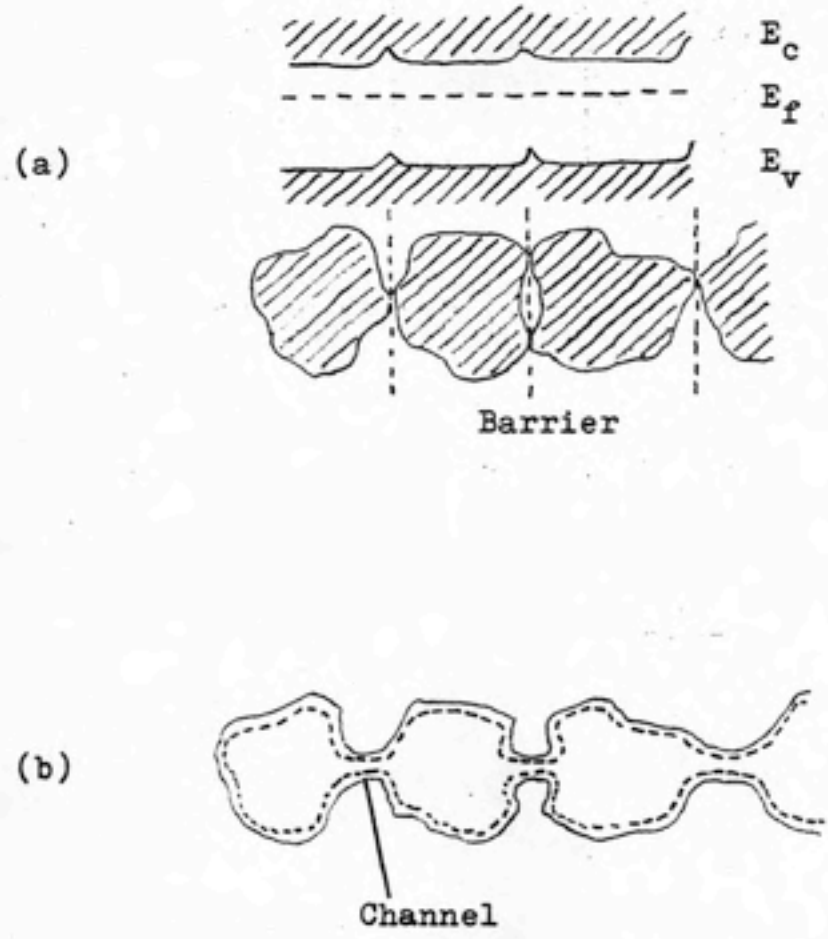

Figure 4. Conductance mechanisms in semiconductor powders
(a) Compressed pellet with barrier formation
(b) Sintered pellet containing electron channels.

volumetric density of electron donors.

The factor before the exponent in Eq. 4 represents the bulk intragranular conductance:

$$\sigma_o = ge\mu n_b \qquad (6)$$

where g is a geometrical factor (0.01 cm for the TGS), e is the electronic charge, μ is the electronic mobility in the space charge region nearest the surface and n_b is the concentration of electrons in the bulk conduction band.

Clifford and Tuma (10) concluded that the TGS bulk conductance results from a native non-stoichiometric defect (an oxygen vacancy) which acts as an electron donor. At steady state, this defect is in equilibrium with the ambient oxygen pressure.

4. TGS 812 relative humidity response

Changes in relative humidity can cause changes in the background conductivity which can make setting alarm levels difficult. Advani and Nanis (2) found that use of the TGS for H_2S detection was limited to relative humidity above 10% because of interference problems below this level.

Relatively little work has been done on evaluating TGS response to water vapor. The manufacturer of the TGS 812 provides a rough plot of relative humidity and temperature dependence in a 1000 ppm isobutane ambient atmosphere (11). This plot is reproduced in Figure 5. Clifford and Tuma (9) found that their results for response to water vapor concentration could be fitted to the empirical equation:

$$R = R_o(1 + K_{H_2O}[H_2O])^{-\beta} \qquad (7)$$

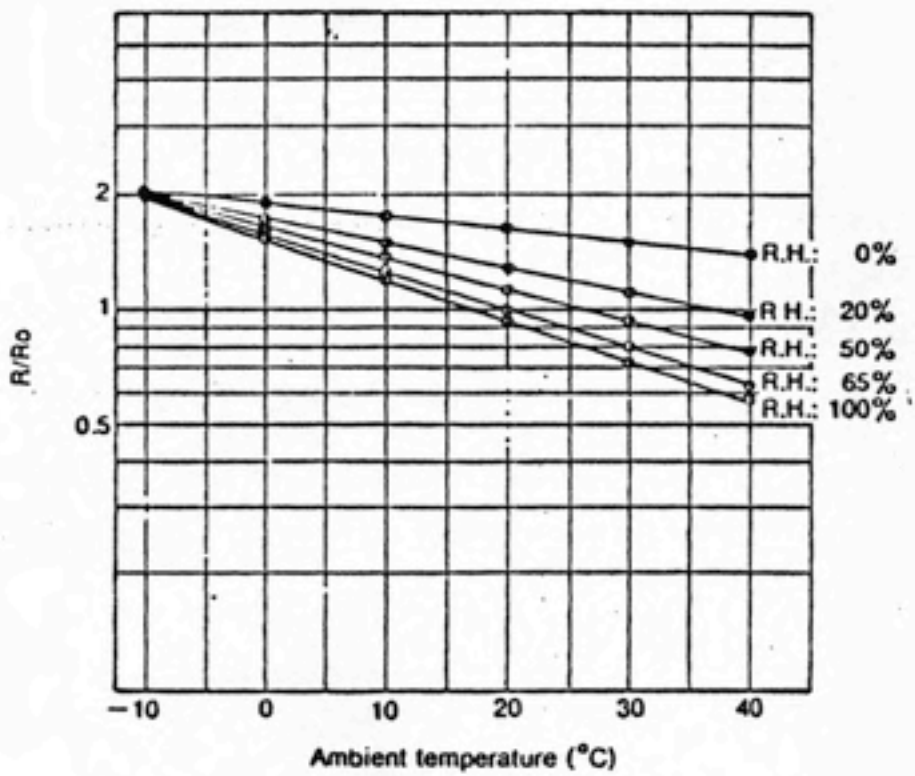

Figure 5. TGS 812 Relative Humidity and Temperature Response

◆ **Test condition:**
VC 10V A.C. / VH 5.0V A.C. / RL 4KΩ

◆ **Remarks:** Ro: Sensor resistance in air containing 1000ppm of Isobutane gas at 20°C and 65% R.H.

R: Sensor resistance in air containing 1000ppm of Isobutane gas at different temperature and humidity.

where R_o is the sensor resistance in ambient air, K_{H_2O} is a constant with respect to water vapor concentration with dimensions of ppm^{-1}, $[H_2O]$ is the concentration of water vapor in volumetric ppm and β is the power law exponent. Clifford and Tuma found values of R_o=151 K , K_{H_2O}=0.0059 ppm^{-1} and β=0.55 for the single TGS 812 sensor they studied. The power law exponent, β, is the slope of the log-log curve of sensor resistance response vs water vapor concentration.

A number of techniques have been suggested for correction of TGS water vapor response. The technique most often used is operation of the sensor at high temperatures. The heating coil in the TGS 812 serves this function. In a study by the National Institute for Occupational Safety and Health (NIOSH) (29), it was suggested that a circuit could be designed so that a reasonably constant water vapor response could be subtracted electronically. This would help eliminate false positives due to water vapor response, but lead to the loss of some sensitivity to organic vapors. Another problem with this technique is that it is limited to uses where water vapor concentration does not vary considerably. Another technique that only partially compensates for relative humidity changes involves the use of a thermistor. This technique, suggested by the TGS manufacturer (11), involves the inclusion of a special temperature-sensitive resistor in the circuit. The resistance of this thermistor changes as the ambient temperature changes. Since ambient relative humidity and air temperature vary in a relatively similar fashion, the response to relative humidity will be somewhat compensated for as the thermistor compensates for seasonal temperature changes.

5. TGS 812 response to single contaminants

The empirical equation for TGS response to water vapor concentration given in Eq. 7 was just one of several developed by Clifford and Tuma (9) for TGS response to single gases. They developed empirical equations for response to oxygen and methane also, as can be seen in Table 1. It should be noted that the power law exponent, β, is the slope of the log-log plot of sensor response versus contaminant concentration. This slope is positive for oxygen and negative for reducing gases. This corresponds to the addition and removal of electrons from the conduction band as described in the discussion of MOS chemisorption. A threshold of detection can be determined from the reciprocal of the constant, ie. $[CH_4] = (K_{CH_4})^{-1}$ (9). The K value can be used as a sensitivity coefficient for comparison between sensors.

Clifford and Tuma (9) used the methane response equation in Table 1 to test the temperature dependence of the TGS response. They found that increasing temperature led to a rapid decrease in K_{CH_4}, ie. rapid sensitivity increase. They found an exponential dependence of K_{CH_4} on inverse absolute temperature. The power law slope, β, becomes slowly steeper with increasing absolute temperature, a directly proportional relationship. This makes changes in concentration easier to detect at high constant temperatures. They found the ambient air resistance, R_o, to have a roughly linear response to temperature change, but only over a narrow temperature range.

Clifford and Tuma (9) found a different response for hydrogen:

$$R = R_o(P_{O_2})^{\beta} (K_o + K_{H_2}[H_2]^2)^{-\beta} \qquad (8)$$

TABLE I.

Clifford and Tuma's Empirical Equations for TGS 812 Single Contaminant Response

Chemical	Equation	Parameter Values Measured
Oxygen	$R=R_0 P_{O_2}^{\beta}$	P_{O_2}=1 (Air) =5 (Pure O_2) β =0.25-0.55
Methane	$R=R_0 (1+K_{CH_4} [CH_4])^{-\beta}$	R_0 =27.4 K K_{CH_4}=4.37 x 10^{-3} ppm^{-1} β = 0.34 (Single sensor) 0.25-0.55 (Range of 10 sensors)
Water vapor	$R=R_0 (1+K_{H_2O} [H_2O])^{-\beta}$	R_0 = 151 K K_{H_2O} = 0.0059 ppm^{-1} β = 0.55

R_0 = Resistance in air

P_{O_2} = Relative partial pressure of oxygen

K_{CH_4}, K_{H_2O} = Constants with respect to the contaminant concentration

β = Power law exponent

The average value of K_{H_2} was 0.12 ppm^{-2}. It is obvious from the squaring factor in this equation that this sensor is very hydrogen sensitive. It is much more sensitive to hydrogen than to methane.

6. TGS 812 general response equation for mixtures

Clifford and Tuma (9) investigated the effects of mixtures of several contaminants on TGS 812 response. The mixtures investigated were:

(1) Carbon monoxide and water vapor

(2) Oxygen, water, carbon monoxide and methane

(3) Methane and hydrogen.

From these mixtures, they were able to develop an empirical equation to describe the general response of the TGS 812 to any combination of reducing gases:

$$(R/R_o)^{-1/\beta} = (1 + \Sigma K_j[G_{1j}]^{n1j}[G_{2j}]^{n2j} \ldots)/[O_2] \qquad (9)$$

where [G] is the reducing gas concentration, n is an integer or fractional integer power and K_j is the sensitivity coefficient for contaminant j.

They state that the proper determination of the power law exponent, β, depends on measuring sensor response to oxygen as well as to the contaminants of interest. They also found this exponent, β, to vary between sensors and to exhibit non-integer exponents. The physical and chemical processes responsible for these last two findings are to be presented in a future paper by Clifford and Tuma.

The mathematical description of TGS response presented in Eq. 9 aids in understanding the competitive and synergistic interactions

among gases in mixtures. It can be seen from Eq. 9 that resistance response depends on a linear combination of individual gas terms. This allows the effects of one gas to be masked by the combined effects of other gases, a competitive interaction. The synergistic interaction occurs when one gas enhances the effect of another. This can be seen in Eq. 9 when the product of several gases constitutes a single term in the summation portion of the equation.

Addition of gas effects in Eq. 9 can be explained by assuming that each term represents a separate reaction for removal of adsorbed surface oxygen (9). This can be demonstrated by the reaction:

$$O_{2g} \underset{K_2}{\overset{K_1}{\rightleftharpoons}} O_{2s} \quad \text{and} \quad n_j G_j + O_{2s} \xrightarrow{K_j} P_j \qquad (10)$$

where O_{2g} is gaseous oxygen, O_{2s} is surface adsorbed oxygen, K_1 and K_2 are exchange rates for oxygen between gaseous (K_1) and adsorbed (K_2) states and G_j is a reducing gas chemically reacting with surface oxygen at rate K_j, yielding a product P_j that is desorbed from the surface. The reducing gas reaction rate constant, K_j, is equivalent to the sensitivity coefficient, K_j, in Eq. 9. For each reducing gas, there will be a different surface reduction equation and reaction rate, K_j.

Watson and Price (48) are also among the limited number of researchers who have investigated TGS response to mixtures. They investigated the response of the TGS 812 to carbon monoxide (CO) and methane (CH_4), both singly and in equal mixtures. They found that the mixture response was overestimated when individual responses to equal concentrations of the two contaminants were added. They concluded that this was due to the non-linear response of the sensor.

7. Limitations of TGS sensors

This discussion of TGS limitations covers TGS sensors in general, but can be applied to the TGS 812 sensor studied in this paper.

TGS sensors must have a stabilization time after first being energized. When the sensor is first turned on, its resistance in clean air drops rapidly and then rises less rapidly to a relatively stable clean air value. This can trigger false alarms in instruments utilizing the sensor. The time to reach the clean air value is known as the primary transitional time or initial action time (13). Ihokura (19) described the mechanism responsible for this phenomenon. The sudden heating of the sensor which occurs when it is first turned on causes momentary excitation of the donor electrons leading to a rapid increase in electron density in the conduction band. This corresponds to the rapid drop in resistance. The slower increase to stabilization corresponds to oxygen adsorption on the sensor surface. The adsorption reaction has a higher activation energy than the electron excitation reaction and is thus a slower process. The primary transitional time was shown by Ihokura to be related to some extent to the amount of doped palladium. The time to stabilization is also a function of the storage time of the unenergized sensor. Generally, the longer the storage time, the longer the initial action time. The TGS 812 reaches its maximum initial action time after 20 days storage. The normal initial action time for the TGS 812 is less than 2 minutes (11). The manufacturer has suggested adding a delayed action circuit to an instrument utilizing the sensor so that these initial false alarms could be avoided (13).

This initial action response is primarily a problem when utilizing

the TGS in hand held instruments which may require immediate response as soon as they are turned on. TGS sensors have another response characteristic known as the secondary transitional period. After long storage in clean air and in some other gases, TGS sensor resistance increases to a maximum of 20% above the stable ambient air value it will eventually reach (13). The resistance reaches its maximum value after six months. The TGS 812 will reach its final, stable ambient value approximately 3 to 6 days after switch-on (11). This secondary transitional period means that no calibrations should be made until the sensor has been switched on for at least one week if the sensor is to be utilized as a long term breakthrough monitor.

The TGS utilized as a breakthrough monitor for organic toxic gases and vapors can encounter interferences from a number of different inorganic gases. These interferences include sulfur dioxide, hydrogen and ammonia. In addition, interference can occur from organic gases such as carbon monoxide. Water vapor interference has been discussed previously. All of these compounds can affect the ability of the sensor to respond accurately to concentrations of a given contaminant of interest.

8. TGS applications

The applications listed here for the TGS sensor cover a variety of TGS models. Applications involving the TGS 812 model studied in this paper are specifically noted.

TGS sensors have been used in domestic gas leak detectors (11,12,13) and fire alarm systems through the detection of smoldering gases such as carbon monoxide (12,13). They have also been used in

systems designed for detection of inflammable gases below their lower explosion limits, LEL (7,49). The TGS 813 was found to work quite well in a prototype permeation indicator for industrial glove testing (46).

Several studies have been done on the use of TGS sensors with respirators, either as breakthrough indicators or in fit testing. Loschiavo (25) attempted to utilize the TGS 812 in fit testing of respirators with ethanol, but found too much interference from the constituents of exhaled breath. The manufacturer (13) lists the application of the TGS 109 in a breath alcohol detector, so Loschiavo's results may be due to choosing the wrong model. A respirator breakthrough indicator for organic vapor respirators was developed by NIOSH (29) and evaluated in another study by Kennedy (22). The circuit for the sensor was designed so that constant humidity readings could be zeroed. The chemicals tested in the Kennedy study were ethyl acetate, tetrahydrofuran, acrylonitrile, methylene chloride and acetone. The alarm response of the indicator was inadequate because readings were not continuous. To conserve the batteries, an eight minute duty cycle was designed. Measurements were only made for thirty seconds out of this eight minutes, thus allowing the possibility for considerable breakthrough before the alarm was set off.

Bratt (6) evaluated the response of the TGS 812 to sixteen contaminants. He developed a prototype respirator breakthrough indicator and tested it against acetone. The response of the TGS 812 over a range of temperature and humidity conditions was also evaluated. The minimum detectable concentrations found by Bratt for the sixteen contaminants over a small range of temperature and humidity conditions are reproduced in Table 2. The contaminant response, temperature and

Table 2

Bratt's Minimum Detectable Concentrations (ppm)

Temperature (Δ°C)†				Chemical	Moisture (Δ% RH)*			
-2	-1	+1	+2		-20	-10	+10	+20
<1	<1	<1	<1	Acetone	<1	<1	<1	<1
2.2	1.1	0.8	1.6	Benzene	5	1	1.2	2.3
2.7	1.2	<1.2	1.9	n-butyl acetate,	5	1.2	1.3	2.8
<1	<1	<1	<1	n-butyl alcohol	1.1	<1	<1	<1
1.6	<1	<1	<1	Carbon tetrachloride	7	<1	<1	1.7
<1.1	<1.1	<1.1	<1.1	Chlorobenzene	1.4	<1.1	<1.1	<1.1
<0.9	<0.9	<0.9	<0.9	1-2 Dichloroethane	1.5	<0.9	<0.9	0.9
1.2	<0.9	<0.9	<0.9	Dichloromethane	2.6	<0.9	<0.9	1.3
<1.4	<1.4	<1.4	<1.4	Methyl alcohol	2	<1.4	<1.4	<1.4
<1	<1	<1	<1	Methyl acetate	<1	<1	<1	<1
<0.7	<0.7	<0.7	<0.7	Methyl ethyl ketone	<0.7	<0.7	<0.7	<0.7
<0.9	<0.9	<0.9	<0.9	Toluene	1.5	<0.9	<0.9	<0.9
<1	<1	<1	<1	1,1,1 Trichloroethane	1.4	<1	<1	<1
2.4	1.1	<1.1	1.5	1,1,2 Trichloroethylene	5.6	<1.1	1.2	2.5
0.9	<0.6	<0.6	<0.6	Vinyl chloride	1.9	<0.6	<0.6	1
<0.4	<0.4	<0.4	<0.4	Xylene	<0.4	<0.4	<0.4	<0.4

†Reference 26°C
*Reference 60% RH

humidity evaluations were all performed utilizing a panel of 22 sensors in a one cubic meter chamber. Bratt's prototype indicator was utilized in this present study.

9. Summary of MOS and TGS literature

Metallic oxide semiconductors (MOS) have shown some promise as sensors for toxic reducing gases. The reducing gases react with an adsorbed oxygen layer on the surface of the semiconductor, releasing electrons to increase the conductivity (lower the resistance) of the MOS. This change in resistance can be measured utilizing an electronic circuit which in turn can set off a preset alarm in response to a given contaminant concentration.

The Taguchi Gas Sensor (TGS) is one of the most common MOS sensors. The TGS 812 model is designed to detect toxic reducing gases. A number of studies have been done on the response of this sensor to single contaminants. It has been found that different contaminants may have different response strengths. Response to hydrogen is much stronger than to most other contaminants such as carbon monoxide.

The sensor can respond to more than one contaminant at a time. The response can be in part due to the presence of an interference such as water vapor. Changes in humidity can make accurate responses to a given contaminant difficult to measure.

A response that is due to the presence of more than one contaminant is very likely to occur. Many chemical exposures in air are to chemical mixtures rather than to a single contaminant. While an increasing volume of research is being done on single contaminant responses, little work has been aimed at response to mixtures.

II. STUDY OBJECTIVE

The objective of this study was to evaluate the effect of solvent mixtures on the ability of an organic vapor detector to be utilized as a breakthrough monitor for a charcoal bed. This was done by placing the detector downstream of a charcoal bed. Comparisons could then be made between the detector response to each single solvent passed through the bed and the response to mixtures of solvents passed through the bed.

III. EXPERIMENT DESCRIPTION

A. METHODOLOGY AND APPARATUS

An apparatus was constructed modeled partially on the work of Bartosh (4) concerning binary vapor effects on respirator service life. This apparatus had several components: a vapor generation system, a charcoal bed, the TGS 812 organic vapor detector and a system for vapor sampling and analysis. A diagram of this system is given in Figure 6.

1. Vapor generation

The solvent vapor was generated by passing a metered amount of air through a Greenburg-Smith impinger packed in ice. The ice ensured that a nearly constant concentration was evolved by maintaining the liquid solvent at a constant temperature. The air containing the vapor was then diluted with a known volume of room air to produce the desired concentration which was delivered to the test chamber containing the charcoal bed.

Pressure regulated house air was passed through a needle valve and rotameter into a Greenburg-Smith impinger. No attempt was made to purify this compressed air, since it was assumed that any contaminants present would be insignificant when compared with the solvents after the large dilution with room air. The metering of the compressed air

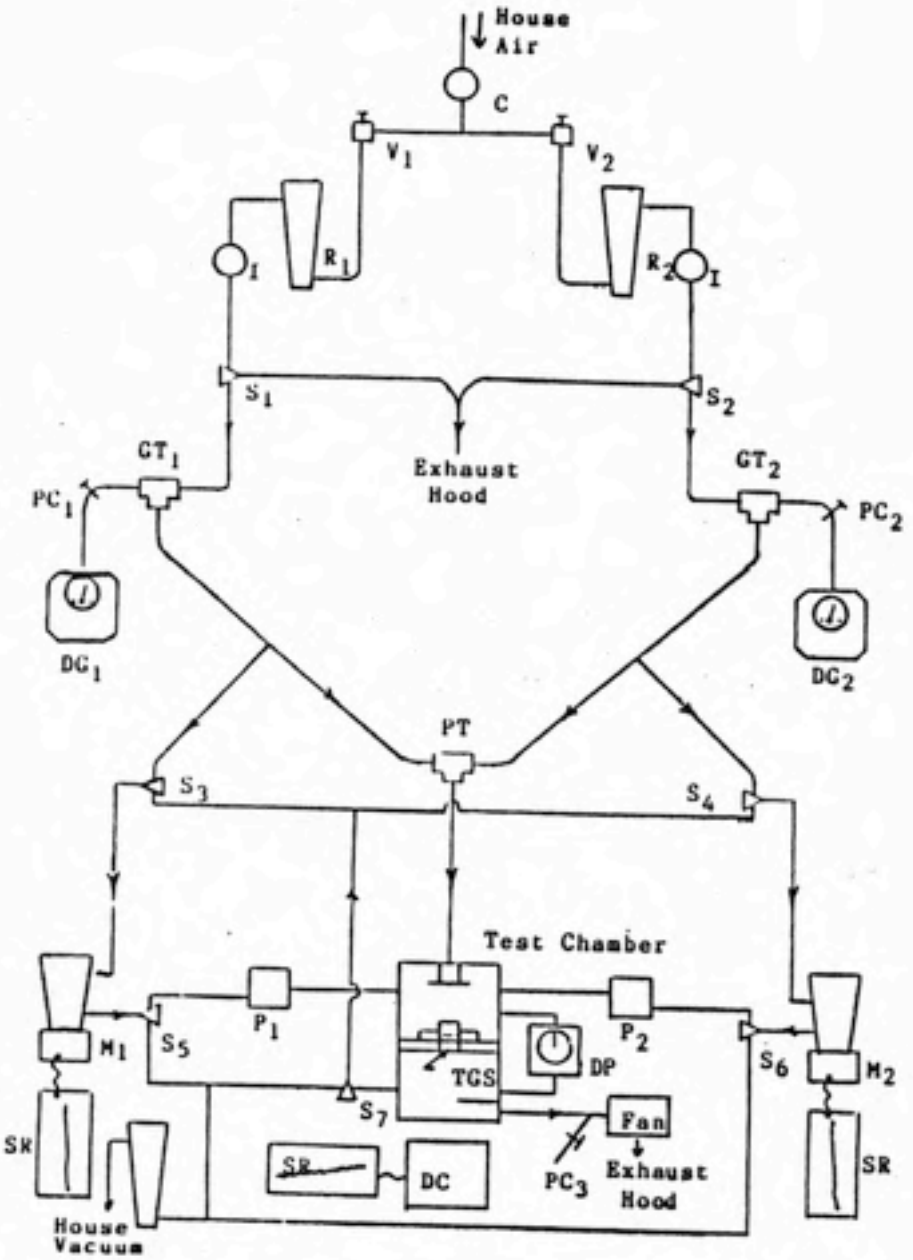

C - Compressed Air
DC - Detection Circuit
DG - Dry Gas Meter
DP - Differential Pressure Meter
GT - Glass Tee (1 inch)
I - Impinger (Greenburg-Smith)
M - Miran Infrared Analyzer
P - Pump (Metal Bellows)
PC - Pinch Clamp
PT - Plastic Tee
R - Rotameter
S - Stopcock (3-way)
SR - Strip Recorder
TGS - Taguchi Gas Sensor
V - Needle Valve

Figure 6. Test Apparatus Diagram

allowed a range of vapor concentrations to be presented to the test chamber.

A one inch glass mixing tee was utilized to mix the vapor from the impinger with the room air. The fresh air flow was measured by a calibrated dry gas meter and was regulated by a pinch clamp on the tubing between the dry gas meter and the mixing tee. Separate systems were utilized for each solvent stream when a mixture of two vapors was to be tested. The separate systems were delivered through another mixing tee to ensure complete mixing before entering the test chamber. A Teflon® 3-way stopcock placed immediately after each impinger allowed the excess solvent vapor to be bypassed to an exhaust hood as needed. Breakthrough times could be determined starting from the time that the stopcock was turned from bypass to straight flow.

2. Cartridge test system with charcoal bed simulation

The cartridge test system consisted of a test chamber, differential pressure gauge and high volume suction fan with a variable voltage supply.

The test chamber was an acrylic cylinder divided into two parts by a center plate containing a cartridge receptacle. The chamber was approximately 20 cm in diameter and 33 cm high with several ports with Swagelok® fittings in the sides of both the top and bottom sections. These ports allowed attachment of a differential pressure gauge across the two sections and attachment of a vapor sampling and analysis system. An entrance baffle encouraged proper mixing and distribution of the airflow. A respirator cartridge holder was set in the middle of the center plate to which another cartridge holder containing the

TGS sensor could be sealed. The differential pressure gauge allowed measurement of the pressure drop across the cartridge and thus could be utilized to determine the integrity of the seals on the chamber and the cartridge. Airflow through the test system was provided by the combination of a high volume suction fan and a house vacuum line attached to the downstream sampling system through a 3-way stopcock. Fan air flow was varied by a rheostat on the suction fan and by adjusting a pinch clamp on the bypass flow to the fan. The house vacuum air flow was controlled through use of a rotameter and a needle valve at the vacuum port.

Activated charcoal packed into an empty respirator cartridge was utilized to roughly simulate a bed of activated carbon of the type found in ventilation gas adsorber systems. A similar procedure was used by Abrams (1) in his evaluation of a recirculating fume hood. The carbon adsorber system chosen to be modeled was the Charcoal Service Corporation "Cinersorb", Model CSC-16-62-AP. This system contained six carbon beds in a frame 24 inches high, 24 inches wide and 16 inches deep with a combined net weight of carbon of 85 lbs. Each of the six beds was 2 inches in depth. The activated carbon was 8 to 16 mesh and was made from a coconut shell base. This system was designed to have a residence time of 0.125 seconds for contact of the airstream with a single charcoal bed (8). The packing density and residence time of the charcoal bed were the key parameters used in simulating this system. The packing density was defined as the ratio of the mass of carbon to the volume of carbon in a single bed. Pulmosan Safety Corporation respirator cartridges were used to model a single bed in the system. A comparison of the adsorber bed and respirator cartridge characteristics

used in the modeling are presented in Table 3.

TABLE 3

Carbon Bed Adsorber Data

	Single Adsorber Bed	Respirator Cartridge
Volume (liters)	18.88	0.145
Mass of carbon (gm)	6.43×10^3	49.4
Residence time (seconds)	0.125	0.125
Packing density (gm/L)	341	341

The flow rate required through the respirator cartridge was 69.6 L/min. The mass of 49.4 gm of carbon was used to produce a packing density of 341 gm/L. The charcoal packed into the respirator cartridges was Fisher Scientific 6 to 14 mesh, coconut shell based activated carbon.

3. TGS 812 organic vapor detection system

The cartridge model described above was set into a specially designed respirator cartridge receptacle containing a TGS 812 sensor. This adapter was in turn set into the receptacle in the divider of the cartridge test system. The electronic circuitry of the breakthrough indicator designed and built by Bratt (6) is shown in Figure 7. A vernier dial on the instrument allowed a concentration limit to be set for instrument response in terms of a reference voltage. The dial was connected to a 20,000 ohm, 10 turn, linear potentiometer. The voltage across this potentiometer was compared with a 10,000 ohm resistor in series with it. On exposure to a concentration, the resistance of the

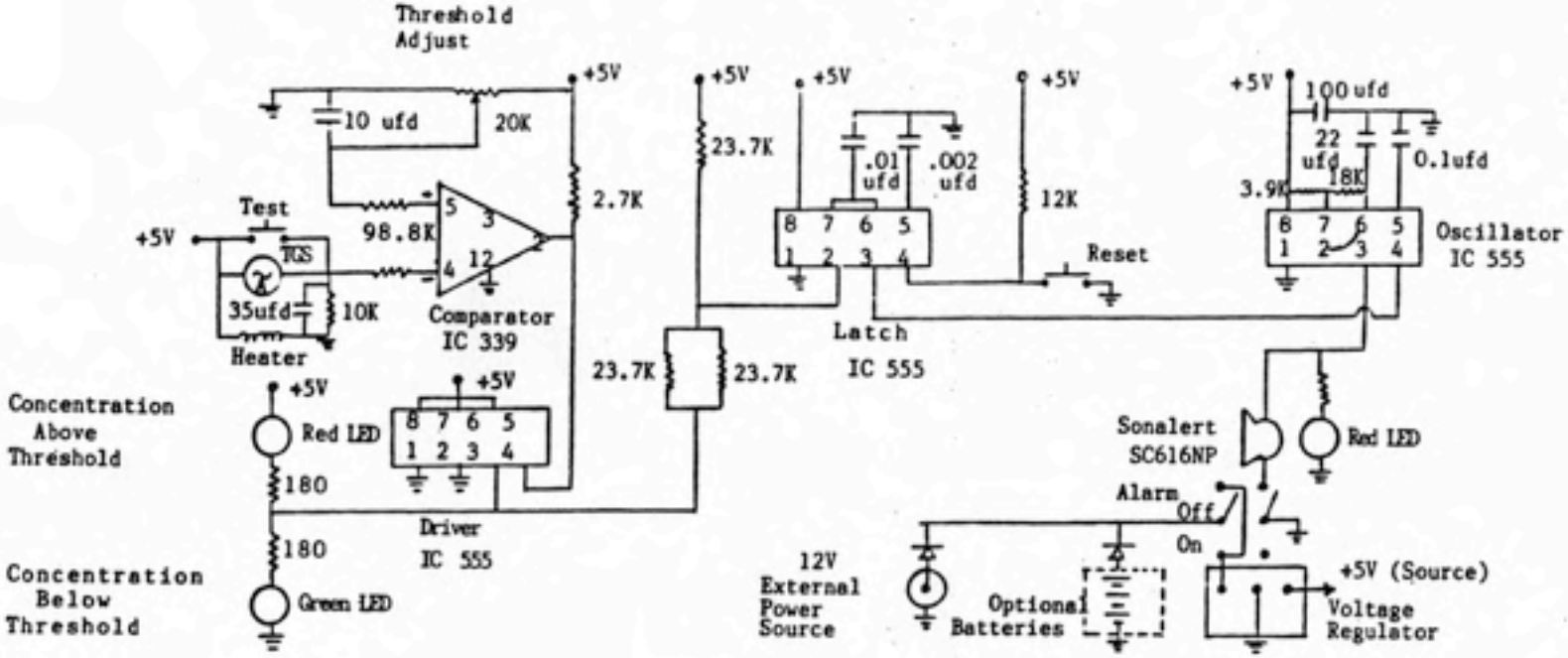

Figure 7. Circuitry Schematic of the Bratt Breakthrough Indicator Device

sensor drops, causing an increase in voltage across the 10,000 ohm resistor. An alarm signal would be generated when this voltage exceeded the pre-set voltage level across the potentiometer.

Voltage for the sensor apparatus was provided by a power supply producing 4.98 VDC.

Since the resistances of the potentiometer and 10,000 ohm resistor are in series, the current through each resistor must be equal. Ohm's Law states:

$$I = V/R \tag{11}$$

where I is the current (amps), V is the voltage (volts) and R is the resistance (ohms).

In terms of the indicator design, the mathematical relationship between voltage and resistance is:

$$\frac{V_{10K\Omega}}{10K\Omega} = \frac{V_S}{R_S + 10\ K\Omega} \tag{12}$$

where $V_{10K\Omega}$ is the dial setting times 0.498 (reference voltage of 0 - 4.98 volts, indicated on a 10-turn vernier dial), V_S is the supply voltage of 4.98 volts, $10K\Omega$ is the known resistance in series with the sensor and R_S is the unknown resistance of the sensor ($K\Omega$).

Substituting the dial setting (DS) for $V_{10K\Omega}$ allows an alarm setting to be made if the sensor has been calibrated. From the calibration plot, the sensor resistance response can be determined for a given concentration and the alarm set by the equation:

$$DS = \frac{100\ K\Omega}{R_S + 10\ K\Omega} \tag{13}$$

The dial setting at which the alarm signals in a clean atmosphere is related to the initial resistance of the sensor. The resistance of the sensor to a known concentration (R_s) can be divided by the resistance in clean air (R_a) for a series of concentrations to develop a calibration curve. In actual use as an alarm system for breakthrough, one need only obtain the clean air resistance (R_a) and consult the calibration plot for the chosen concentration to obtain the R_s value to calculate the dial setting (DS) needed.

To establish a permanent record of sensor response in this study, a strip chart recorder was connected across the sensor. With this connection, the calculation of sensor resistance (R_s) took the form:

$$R_s = \frac{10\ K\Omega}{V_s/V_m - 1} \qquad (14)$$

where V_m is the voltage measured across the sensor.

4. Vapor sampling and analysis system

The sampling system was designed so that it was possible to sample in a closed circuit system upstream of the cartridge or to sample downstream with the sample then being exhausted. The solvent vapor used to challenge the cartridge could be routed through a MIRAN infrared analyzer and back into the chamber through a bellows pump. Total air flow and mass balance were not affected using this method.

The house vacuum system could be utilized to draw a sample from the downstream section of the cartridge chamber through a MIRAN analyzer. The flow rate for this sampling method was controlled through use of a needle valve and a rotameter. A higher sampling rate than that used with upstream bellows pumps allowed a much shorter meter

response time. A bypass was placed on this downstream sampling line so that constant air flow could be maintained when no downstream sampling was performed.

B. SOLVENTS

The solvents chosen for use in this study were: acetone, toluene and carbon tetrachloride. All three were ACS certified reagent grade. Preliminary testing of the sensor showed no detectable response to carbon tetrachloride even with concentration increments of 100 ppm. Carbon tetrachloride has a 1984 ACGIH Threshold Limit Value (TLV) of 5 ppm (3). Carbon tetrachloride was therefore eliminated from further testing. Chemical and physical data on acetone and toluene are presented in Table 4.

C. PROCEDURE

The following procedures were performed for acetone and toluene: determination of suitable analytical wavelengths for the MIRAN infrared analyzers, calibration of the MIRAN analyzers at the chosen wavelengths, tests of each of the single components, tests of the binary mixture, sensor response calculation and determination of charcoal characteristics. The TGS 812 sensor was energized in room air for two weeks before the first experimental run.

1. Determination of suitable analytical wavelength

Infrared analysis depends in part on the ability of different

TABLE 4

Solvent Characteristics

	Solvent		
	Acetone	Toluene	Reference
Formula	CH_3COCH_3	$C_6H_5CH_3$	50
Family	Ketone	Alkyl Benzene	31
Synonym	2-Propanone	Methyl Benzene	50
Molecular Weight (g^m/mole)	58.08	92.15	50
Density (g^m/cm^3)	0.7899	0.8669	50
Vapor Pressure (Torr @23°C)	210.9	25.6	30
Dipole Moment (Debyes)	2.88±1%	0.36±5%	50
Boiling Point (°C)	56.2	110.6	50
Nelson constant			31
a	0.034	0.12	
b	0.0029	0.0024	
Threshold Limit Value, 1983 (ppm)	750	100	3
Permissible Exposure Limit (ppm)	1000	200	35

chemical functional groups to absorb infrared radiation at specific characteristic wavelengths. When analyzing a mixture of chemicals, it is important to determine separate wavelengths where maximum absorbance response can be determined for each component without interference from the other component. The MIRAN manufacturer, Foxboro Analytical, publishes a list of wavelength settings for maximum response for contaminants listed in the 1982 Threshold Limit Value booklet published by the American Conference of Governmental Industrial Hygienists (15).

The spectral range of the MIRAN can be scanned automatically. Scans of room air and house supplied air were made with readings charted on a percent transmittance scale. These charts were compared with individual scans made for acetone and for toluene at concentrations of approximately 250 ppm each. The wavelength settings suggested by Foxboro Analytical were examined on each plot to determine if possible interferences existed for individual contaminant measurements when analyzing the binary mixture. These contaminant scans were accomplished by injection of sample aliquots into a closed loop system utilizing a metal bellows pump and Teflon® tubing. The assumption was made that injected liquids are vaporized completely and that these vapors behave as ideal gases. To determine the volume of injected liquid needed to achieve 250 ppm, the ideal gas laws were used. The molar volume of the test contaminant was calculated from the relationship:

$$MV = (RT/P)(1000) \qquad (15)$$

where MV is the molar volume (cm^3/mole), R is the ideal gas constant [(62.361 liter-mm Hg)/(g-mole-^oK)], T is the system temperature (^oK), P is the system pressure (mm Hg) and 1000

is a conversion factor from liters to cm^3.

The volume of liquid needed for injection was then calculated from the relationship:

$$n = \frac{(250\ ppm)(MW)(5640)(10^{-3})}{(\rho)(MV)} \qquad (16)$$

where n is the injection volume (microliters), MW is the molecular weight of the test contaminant (gm/mole), the value 5640 represents the closed loop volume (cm^3), 10^{-3} is the conversion factor from cm^3 to microliters and ρ is the density of the liquid solvent (gm/cm^3).

2. Calibration of the MIRAN spectrometers

Once a wavelength free of interference between test contaminants and atmospheric components was found, calibration of the MIRAN for each contaminant was begun. The MIRAN calibration requires the setting of a pathlength which would give an absorbance less than 1.0 at the maximum test concentration. From Beer's Law, the following relationship between absorbance (A) and pathlength (L) occurs:

$$A = CL\varepsilon \qquad (17)$$

where C is contaminant concentration (ppm) and ε is an extinction constant ($ppm^{-1}\ m^{-1}$).

This equation can be rearranged to:

$$\varepsilon = \frac{A}{CL} \qquad (18)$$

By inserting the values obtained for the test contaminant from the previously mentioned Foxboro list (15), the extinction constant can be determined. This value is then inserted into an equation suggested by

Reist (38) to determine the correct pathlength required for MIRAN analysis:

$$L = \frac{0.3}{C\varepsilon} \qquad (19)$$

where 0.3 is the absorbance value suggested by Reist (38) and C is the median of the calibration concentrations.

The MIRAN pathlength was adjusted to the pathlength setting closest to the calculated value.

A calibration curve for each contaminant was developed by successive injections into the closed loop calibration system. The absorbance value produced two minutes after each injection was measured. These values were plotted against the cumulative concentration. The concentration increment (C) for each injection was calculated from a rearrangement of Eq. 16:

$$C = \frac{(n)(\rho)(MV)(10^6)}{(MW)(5640)} \qquad (20)$$

The system was purged and several concentrations were remeasured. This calibration procedure was followed for both test contaminants and both MIRAN analyzers.

3. Tests of single contaminants

In the single contaminant tests, one MIRAN was utilized to monitor the upstream challenge concentration. The other MIRAN monitored downstream concentrations to determine breakthrough. This downstream MIRAN response also served as the concentration comparison when determining TGS 812 response to the contaminant. The stopcocks in the sampling system were adjusted so that a sample was drawn out of the

downstream section of the test chamber through the MIRAN and then out of the system through the house vacuum. The rotameter connected to the house vacuum was set to achieve a 20 L/min flow rate to allow a fast response time for the downstream MIRAN. The residence time of 0.125 seconds given for the carbon adsorber bed was divided into the volume of the respirator cartridge, 0.145 liters, to find a flow rate of 69.6 L/min. Once this flow rate (Q) was known, the approximate flow rate (Q_i) required through the Greenburg-Smith impinger could be estimated from the relationships:

$$C \cdot Q = \Sigma C_i \cdot Q_i \qquad (21)$$

and

$$C_i = (P/P_i)(10^6) \qquad (22)$$

where C_i is the concentration (ppm) at flow rate Q_i (L/min) in stream i , C is the concentration of vapor (ppm) at total flow rate Q (L/min), P_i is the partial pressure of the solvent vapor (mm Hg) and P is atmospheric pressure (mm Hg). From these two equations the flow rate, Q_i, through the impinger can be derived:

$$Q_i = \frac{(C)(P)(69.6\ \text{L/min})}{(P_i)(10^6)} \qquad (23)$$

It should be noted that the solvent vapor pressure, Pi, was found for temperatures near 0 °C to 4 °C due to use of the ice bath to maintain impinger temperature. The concentration value, C, was set to the desired challenge concentration for this calculation.

The flow through the rotameter and impinger was adjusted to the value of Q_i via a needle valve on the house air. The stopcock was adjusted to exhaust the vapor before it reached the cartridge chamber

during the setup procedure. The flow through the dry gas meter was adjusted to a value of 69.6 - Q_i. This was accomplished through adjustment of a pinch clamp on the tube between the meter and the glass mixing tee and through adjusting the bypass clamp and rheostat on the exhaust fan. During adjustments of flow rates in all experimental trials, a setup cartridge was utilized containing 49.40 gm of the Fisher activated charcoal.

After the initial flow setup, the exhaust fan was shut off. A fresh respirator cartridge containing the pre-weighed amount of charcoal was placed in the cartridge chamber and the chamber sealed. Modeling clay provided a further seal around the cartridge after it was screwed into the receptacle. The fan was turned on again and allowed to pull air through the cartridge for 5 to 10 minutes to establish a baseline reading for TGS response to uncontaminated air, R_a. The flow rate was adjusted, if necessary, during this period.

After a steady baseline was established, the strip chart recorders connected to each MIRAN were turned on and the stopcock turned to route vapor into the system. The test was continued until the downstream concentration reached half of the upstream challenge concentration. The breakthrough times to achieve 10% (t_{b10}) and 50% (t_{b50}) of the challenge concentration were noted. Depending on the challenge level, times for breakthrough at the following concentrations were also noted: 1, 5, 10, 25, 50, 100, 150, 200, 250 and 500 ppm. These breakthrough times were utilized later in developing TGS sensor response curves. Relative humidity, room temperature and cartridge pressure drop readings were noted.

4. Tests of the binary mixture

For binary vapor tests, each MIRAN was assigned to monitor one of the mixture components. The same MIRAN was utilized for both upstream and downstream monitoring of its assigned component.

The flow rate needed for each of the impingers was determined utilizing Eq. 23. The concentration, C, was set to the concentration value desired for the component at a flow rate, Q, in the mixed stream of 69.6 L/min. The pinch clamps on each of the dry gas meter lines were utilized to produce the desired ratio of concentrations in the mixture. Adjustments were made to provide mixtures with similar concentrations of each component at low, medium and high exposure ranges (approximately 250 ppm, 500 ppm and 1000 ppm). This was accomplished by adjusting each pinch clamp to provide $34.8 - Q_i$ L/min, where 34.8 L/min is half of the system flow rate of 69.6 L/min. A setup cartridge was utilized during these adjustments. After setup, the fan was shut off, a fresh cartridge of pre-weighed charcoal was placed in the chamber and the chamber was sealed. The fan was turned on again and further adjustments to airflow were made as needed while the TGS response baseline for uncontaminated air was established as in the single contaminant test. Solvent vapors were routed to the exhaust hood while setup procedures were followed.

Once a TGS baseline was established, the strip chart recorder for each MIRAN was turned on and the stopcocks for each contaminant were turned to deliver the solvent vapors to the system.

The bellows pumps utilized for upstream sampling had a much slower sampling rate than the 20 L/min for downstream sampling. If an attempt was made to measure upstream concentrations at the beginning of an

experimental run, it could be possible to miss the 10% breakthrough due to the slower sampling rate and required purge time due to the higher challenge concentration. For this reason, each MIRAN was set to monitor downstream concentrations at the beginning of each run. The run was allowed to continue until nearly 50% of the desired challenge concentration had broken through for the component having the higher charcoal retention. At this point the stopcocks were routed to allow sampling of the upstream challenge concentrations. The flow rates were continually monitored to assure that the measured challenge concentration had been maintained throughout each experimental run. Room temperature, relative humidity and cartridge pressure drop were noted.

When determining any breakthrough time, the assumption was made that there was a delay in response of either MIRAN because time was needed to fill the 5640 cm^3 volume of the MIRAN sampling cell. Bartosh (4) found that 95% of the true response was achieved by the MIRAN after 51 seconds. Since this current project utilized the same sampling flow rate of 20 L/min in a similar downstream sampling system, this 51 second response delay was corrected for in determining breakthrough times.

5. Sensor response calculations

TGS 812 sensor response curves for each experimental run were developed by noting the voltage reading measured across the sensor, V_m, at each of the corrected breakthrough times. This value was inserted in Eq. 14 to determine the sensor resistance, R_s, at that breakthrough time. The fresh air resistance value, R_a, for each experimental

run was determined from the baseline reading taken at the beginning of that run.

Once the R_a value and all R_s values for an experimental run had been determined, a TGS 812 response curve could be generated.

For the single contaminant tests, the ratio R_s/R_a was plotted against the contaminant concentration at each defined breakthrough point (ie. 1 ppm through 500 ppm) as well as the 10% and 50% breakthrough concentrations.

The procedure for mixtures assumes that each component will contribute to the sensor response at any given point in time. It thus becomes important to know both concentrations at any breakthrough time of either one of the components. At a corrected breakthrough time for component A readings were taken for the TGS 812 voltage value and concentration of component B. The procedure was repeated for all designated breakthrough times for both components. The R_s and R_a calculations were performed as in the single contaminant tests and the ratio R_s/R_a found for all breakthrough points.

It should be possible to visualize the response trend of the TGS 812 to the presence of a two component mixture utilizing a 3-dimensional plot with R_s/R_a as the dependent value. In addition, the equation developed to produce this plot should allow estimates to be made of sensor response to any concentrations of the two components within the measured range.

6. Determination of charcoal characteristics

The Fisher activated carbon was evaluated to determine bulk density, specific bulk volume, total void volume and solid volume of

the granules utilizing methods described by Bartosh (4).

Bulk density was determined by vibrating a pre-weighed (49.401 gm) sample of the carbon in a volumetric flask to a minimum volume. The charcoal mass was divided by this minimum volume to obtain the bulk density. Specific bulk volume was found by taking the reciprocal of the bulk density. Total void volume was found by adding water to this same sample to more than cover the charcoal. The volume of water added was noted and the flask was agitated and allowed to settle several times over the course of two hours. At the end of this time, the original charcoal volume was subtracted from the total volume of the mixture. The difference was then subtracted from the total amount of water used and the difference divided by the mass of charcoal used to obtain the total void volume. The total void volume was then subtracted from the specific bulk volume to obtain the volume of the solid granules.

The adsorption capacity of the charcoal at the 10% breakthrough point was also determined for each of the single contaminant tests. To determine these capacities, the challenge concentrations had to be converted from ppm to mg/L:

$$C_m = C_p(MW/MV) \qquad (24)$$

where C_m is the concentration in mg/L, C_p is the concentration in ppm, MW is the molecular weight of the test contaminant (gm/mole) and MV is the molecular volume in cm^3/mole.

The total flow rate in L/min, Q, for each experimental run was then used to calculate the total challenge rate, CR, in gm/hr:

$$CR = (C_m)(Q)(60min/hr)/(1000mg/gm) \qquad (25)$$

The mass of solvent vapor which escaped through the charcoal bed

up to the 10% breakthrough point was determined by a strip chart paper weighing procedure. A solvent challenge mass in grams, M_{SC}, was calculated:

$$M_{SC} = (CR)(t_{10\%})/(60) \quad (26)$$

where $t_{10\%}$ is the 10% breakthrough time (min.) and 60 is a conversion factor from minutes to hours.

A "standard" piece of strip chart paper was generated by tracing a straight line for a length equivalent to one hour at the absorbance value corresponding to 10% of the challenge concentration. This tracing was then cut out and weighed to find a "standard" chart paper mass, M_{SP}. A "standard" mass, M_{SS}, for solvent escaping through the charcoal at 10% of the challenge rate over one hour was calculated. The chart paper for the experimental run was cut along its reading trace up to the 10% breakthrough point and weighed to find the breakthrough paper mass, M_{BT}. The total mass, M_{ES}, of solvent escaping through the charcoal bed up to the 10% breakthrough point was then determined:

$$M_{ES} = (M_{BT})(M_{SS})/(M_{SP}) \quad (27)$$

The mass of solvent adsorbed, M_A, was found by subtracting the escaped solvent mass, M_{ES}, from the solvent challenge mass, M_{SC}, found in Eq. 26.

The adsorption capacity was found by dividing the mass of solvent adsorbed, M_A, by the mass of charcoal in the respirator cartridge, M_C, in each experimental run.

The experimental design allowed data to be collected regarding carbon adsorption as well as TGS response. The breakthrough times measured in each single contaminant test were compared against results

predicted by two equations described in Appendix A, Eq. 29 developed by Nelson and Correia (31) and Eq. 31 adapted by Abrams (1) from Grubner and Burgess (16).

IV. RESULTS AND DISCUSSION

A. TGS 812 RESPONSE CHARACTERIZATION

The objective of this study was to characterize the response of the TGS 812 sensor to a binary solvent mixture which had been passed through a charcoal bed. To accomplish this, the response to each single contaminant was first characterized. Table 5 contains the response values at six selected concentrations for each single test.

1. TGS 812 single contaminant response

Acetone and toluene were the two solvents tested in this study. These two solvents were also evaluated for TGS 812 response in a study by Bratt (6). Bratt designed and built the prototype breakthrough detector utilized in this current study. It was expected that response characteristics would be similar in the two studies. This expectation did not hold true.

The TGS response curves for acetone in Trials 1 - 4 are presented in Figures 8 to 11. All data points from these tests are plotted together in Figure 12. The straight line in Figure 12 represents the power function equation derived from a least squares regression of all data points in the acetone trials:

$$TGS = (1.135)\ C_A^{-0.228} \qquad (28)$$

where TGS is the TGS 812 response (R_s/R_a) to acetone and C_A

TABLE 5

TGS 812 Response (Rs/Ra) in Single Vapor Tests

Trial Number	Challenge Concentration (ppm)	Concentration (ppm)					
		1	10	50	100	250	500
1-A	119.3	0.944	0.738	0.464	---	---	---
2-A	617.2	0.966	0.700	0.439	0.372	0.269	---
3-A	1062.7	0.983	0.899	0.684	0.569	0.387	0.300
4-A	1110.1	0.848	0.682	0.450	0.374	0.259	0.224
5-T	904.1	1.000	0.982	0.934	0.824	0.800	0.762
6-T	347.7	0.740	0.926	0.946	0.946	0.844	---
7-T	263.8	0.629	0.712	0.643	0.634	---	---
8-T	1386.6	0.921	1.000	0.890	0.882	0.587	0.647

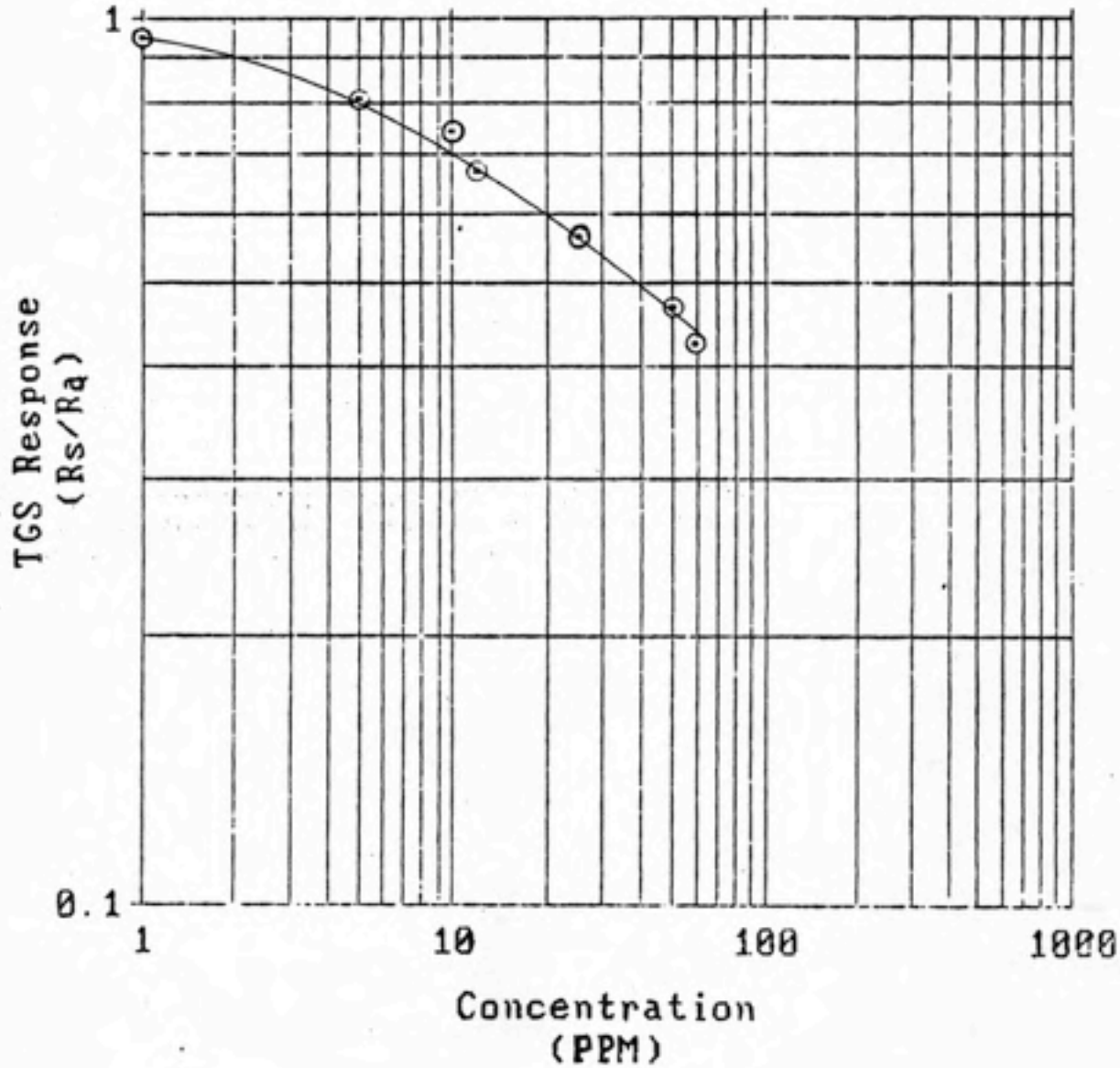

Gartland's TGS Acetone Data
Trial 1

Figure 8

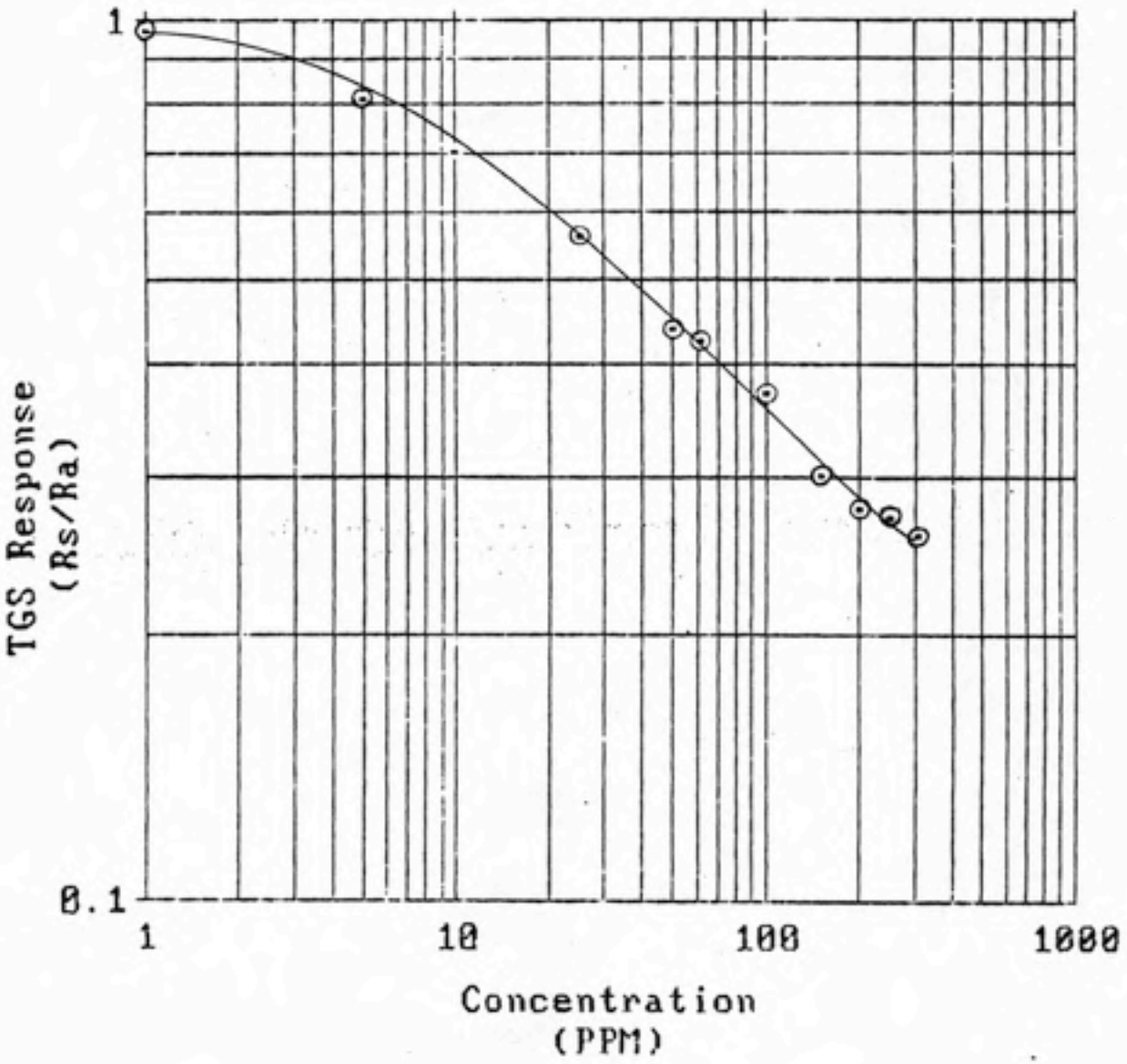

Gartland's TGS Acetone Data
Trial 2

Figure 9

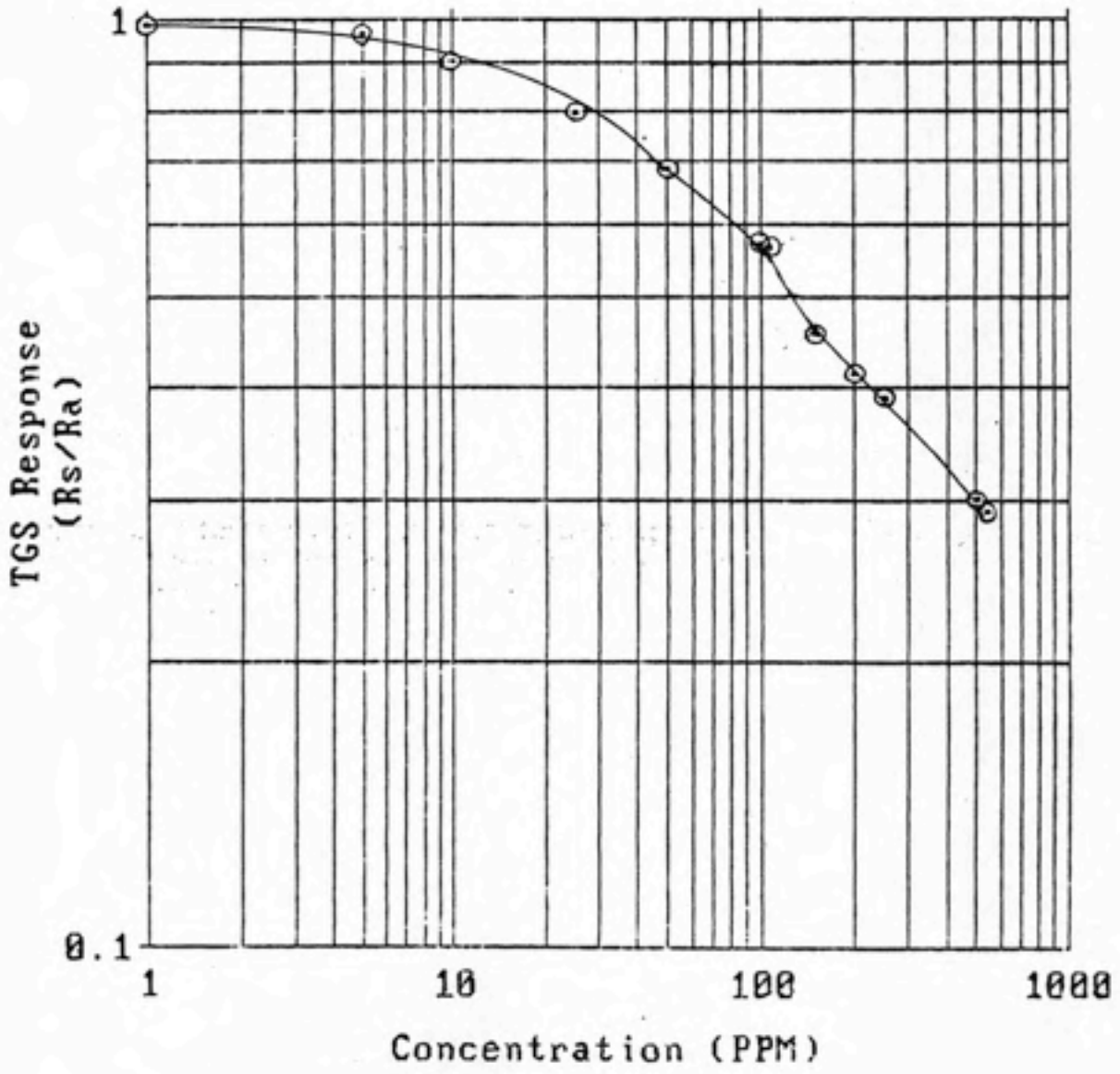

Gartland's TGS Acetone Data
Trial 3

Figure 10

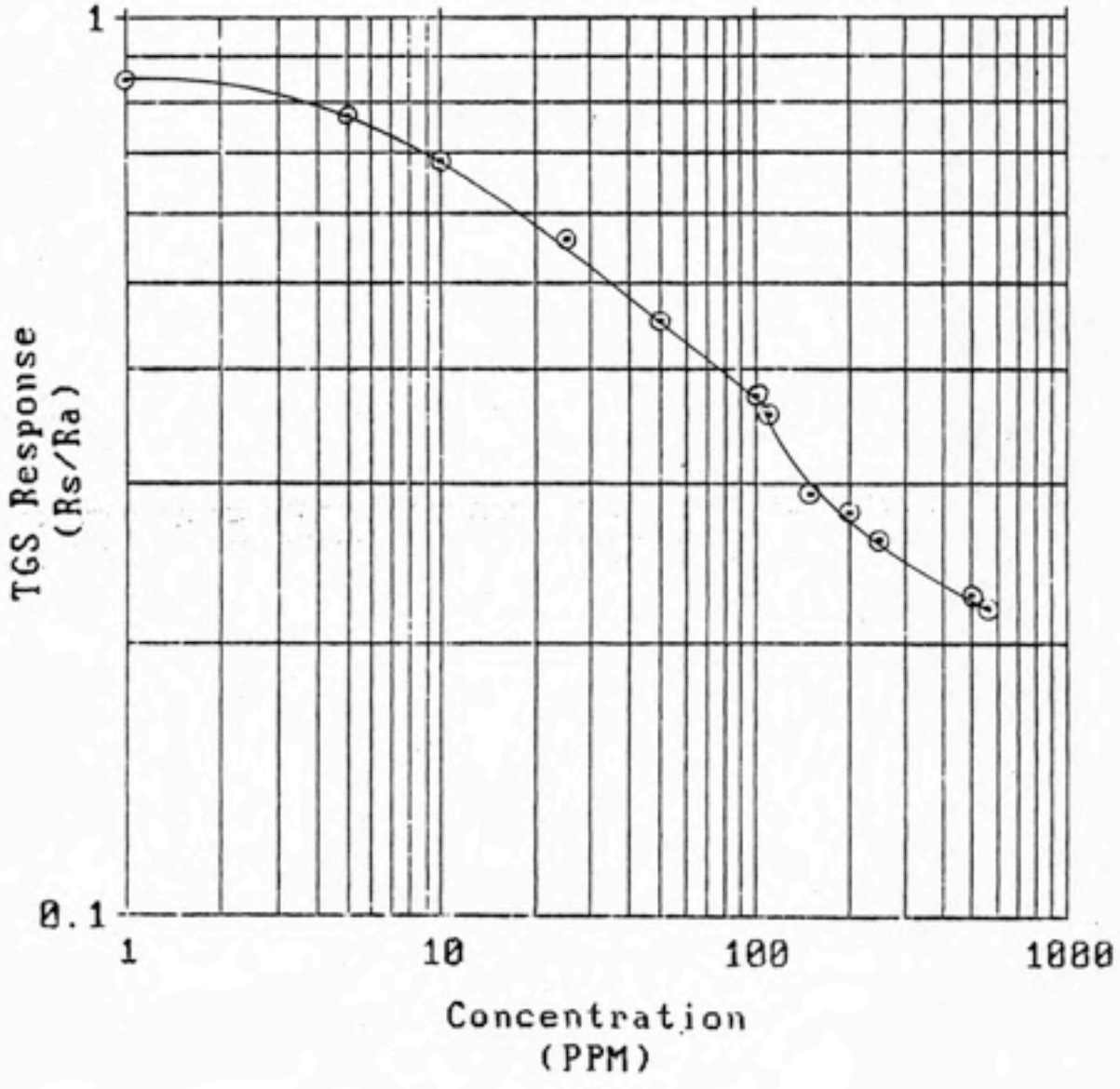

Gartland's TGS Acetone Data
Trial 4

Figure 11

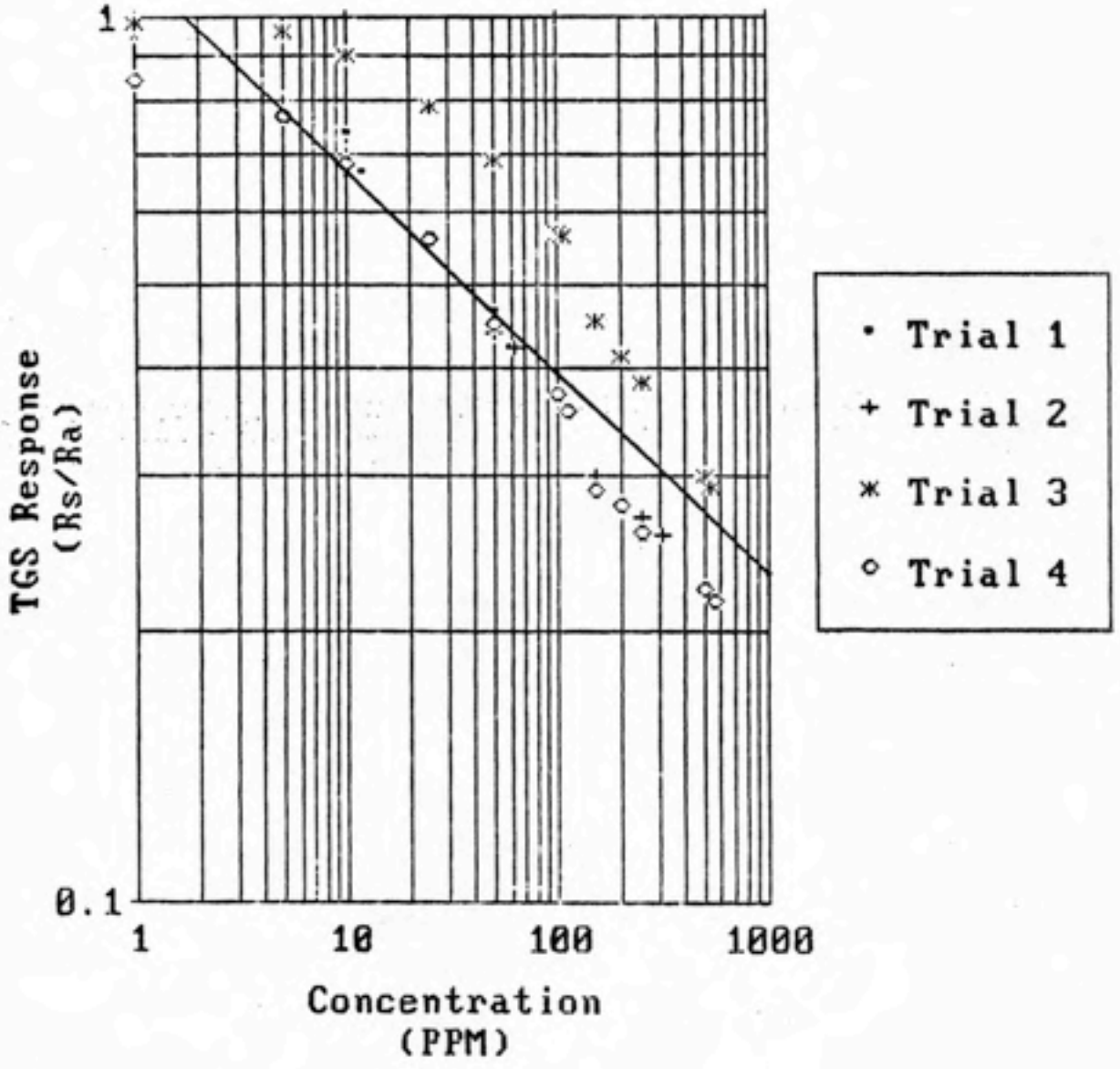

TGS Acetone Calibration Curve
(Gartland's Data)

Figure 12

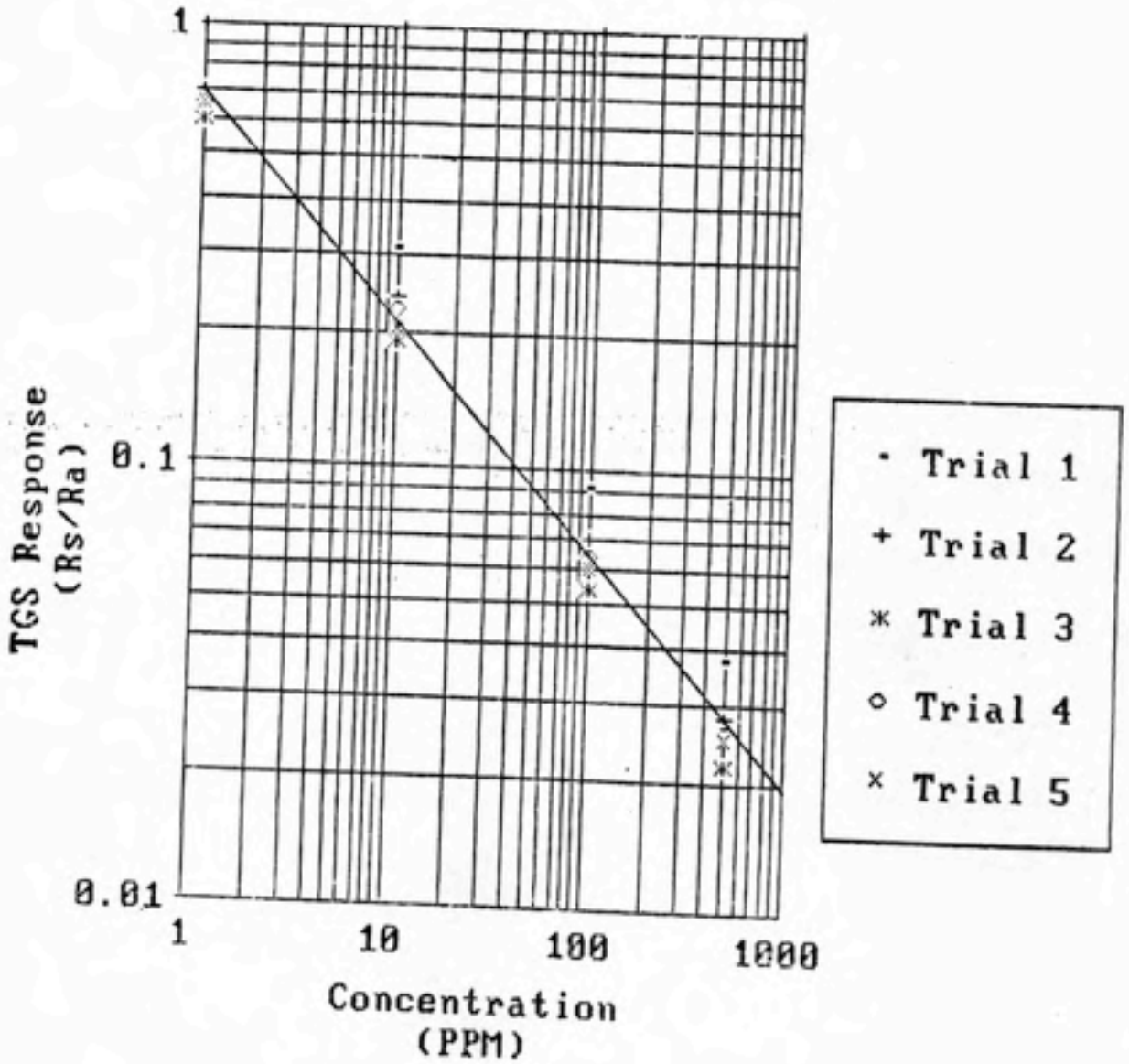

TGS Acetone Calibration Curve
(Bratt's Data)

Figure 13

is the acetone concentration (ppm).

A correlation coefficient (R^2) of 0.840 was obtained. It can be seen that below 10 ppm the relationship tended to be more exponential.

A plot of the results of Bratt's (6) acetone calibration tests is presented in Figure 13. It can be seen that the response in his tests was much stronger. The sensitivity to changes in concentration was much greater also as is evidenced by the greater slope found in the least squares regression of Bratt's acetone data:

$$TGS = (0.7035)\ C_A^{-0.519} \qquad (29)$$

The TGS 812 response curves for toluene in Trials 5 - 8 are presented in Figures 14 through 17. All data points from these points are plotted together in Figure 18. A power function equation for toluene response was developed and is represented by the straight line in Figure 18:

$$TGS = (0.879)\ C_T^{-0.020} \qquad (30)$$

where C_T is the toluene concentration (ppm).

A correlation coefficient (R^2) of 0.053 was obtained. It is evident that the toluene data does not follow a power relationship. An examination of Figure 18 shows that no discernable response to toluene occurs below 100 ppm.

A plot of the results of Bratt's (6) toluene calibration test is presented in Figure 19. As with the acetone tests, response to toluene is much greater in Bratt's test. A least squares regression of his data is represented by the straight line in Figure 19 and the following equation:

$$TGS = (0.9018)\ C_T^{-0.474} \qquad (31)$$

Comparison of Figures 18 and 19 and the slopes in Eq. 30 and Eq.

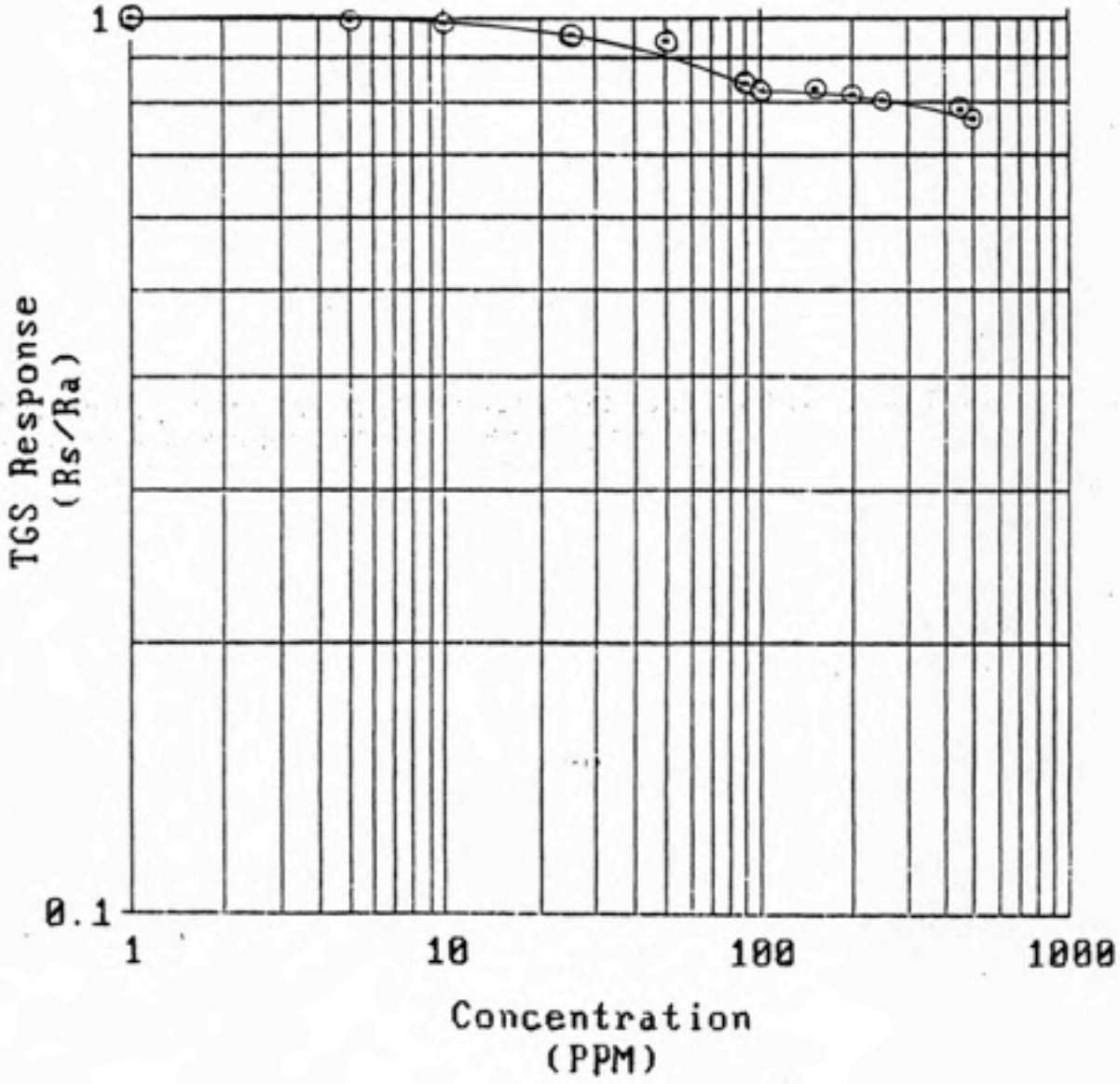

Gartland's TGS Toluene Data
Trial 5

Figure 14

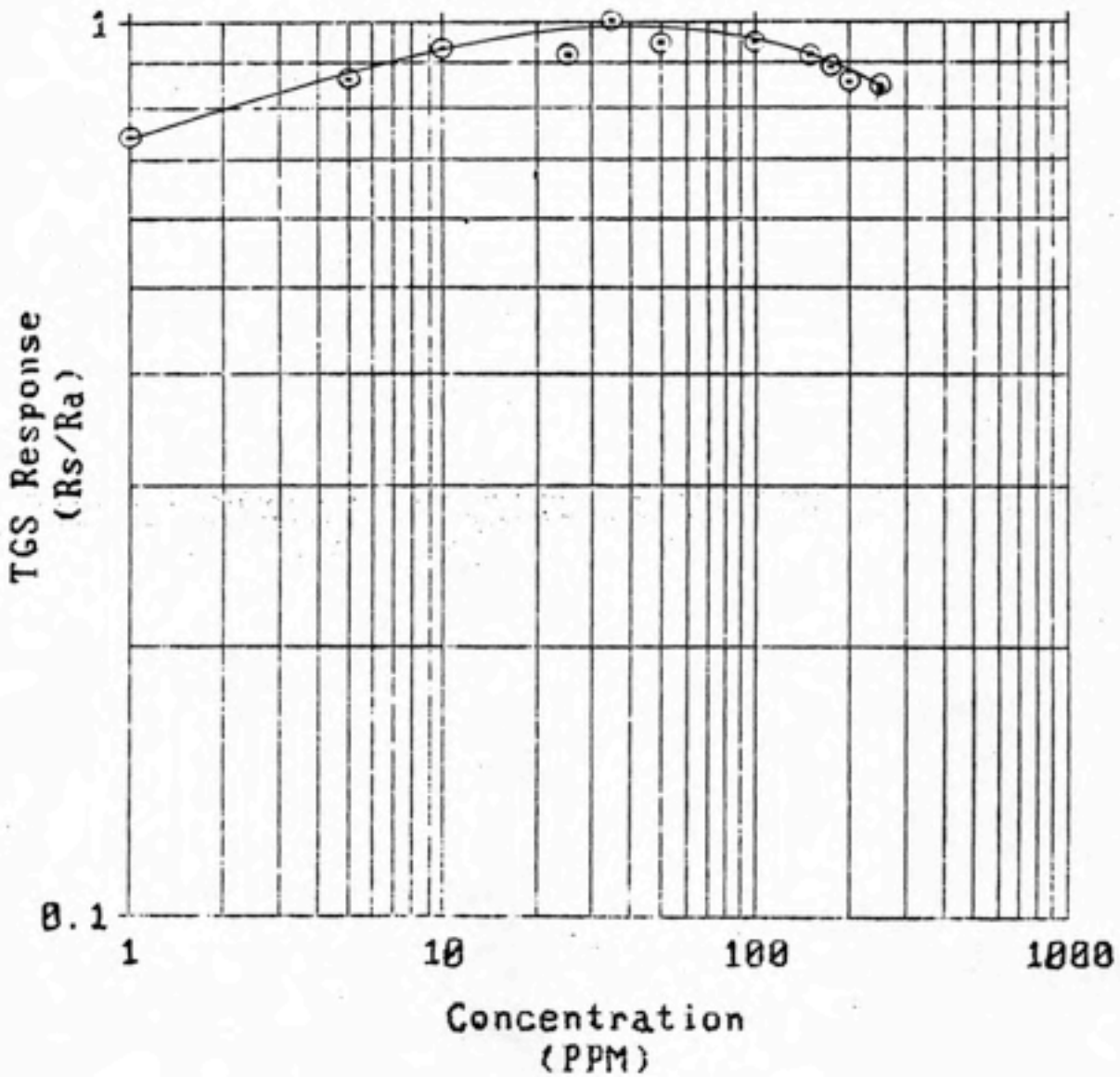

Gartland's TGS Toluene Data
Trial 6

Figure 15

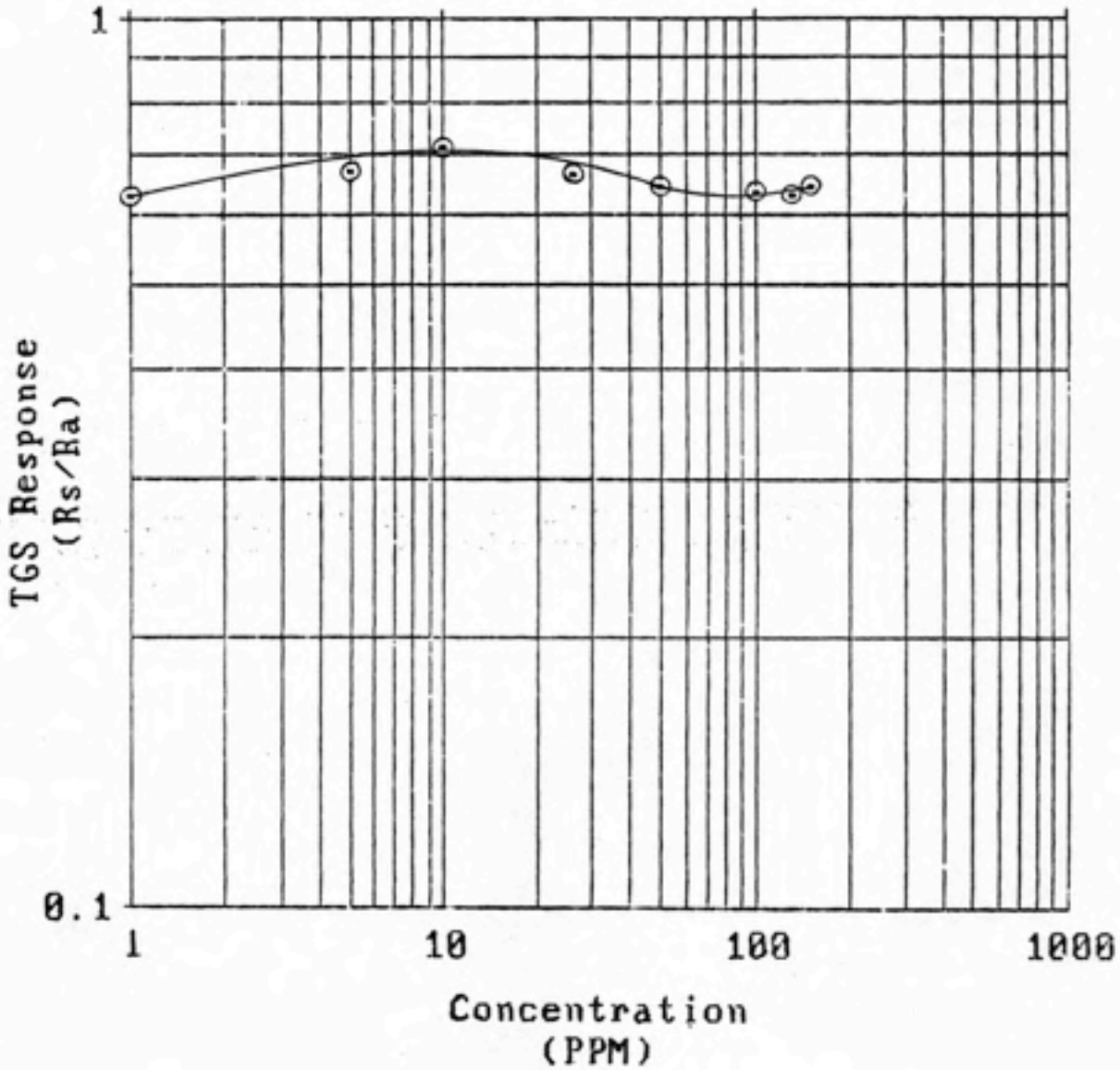

Gartland's TGS Toluene Data
Trial 7

Figure 16

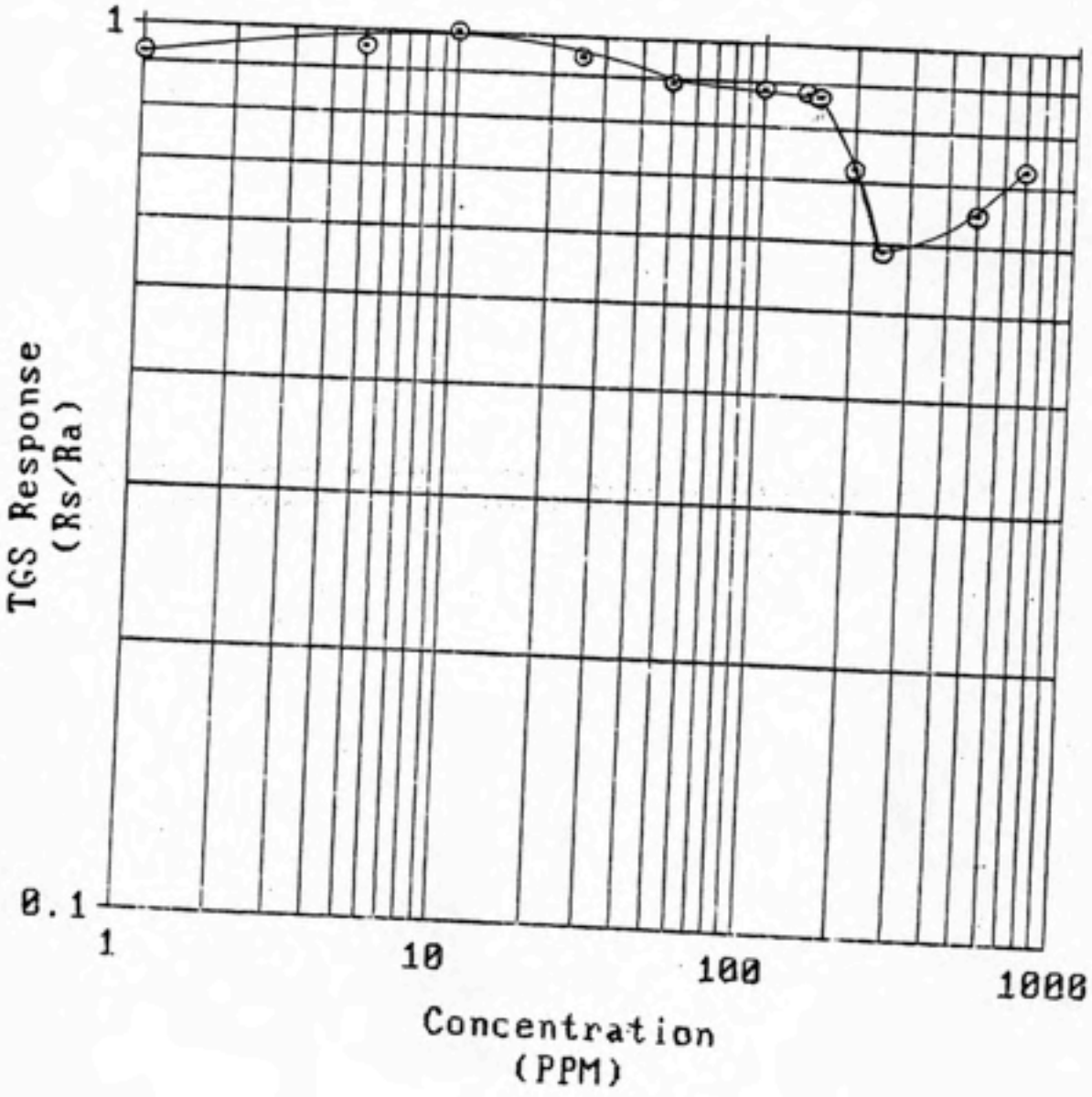

Gartland's TGS Toluene Data
Trial 8

Figure 17

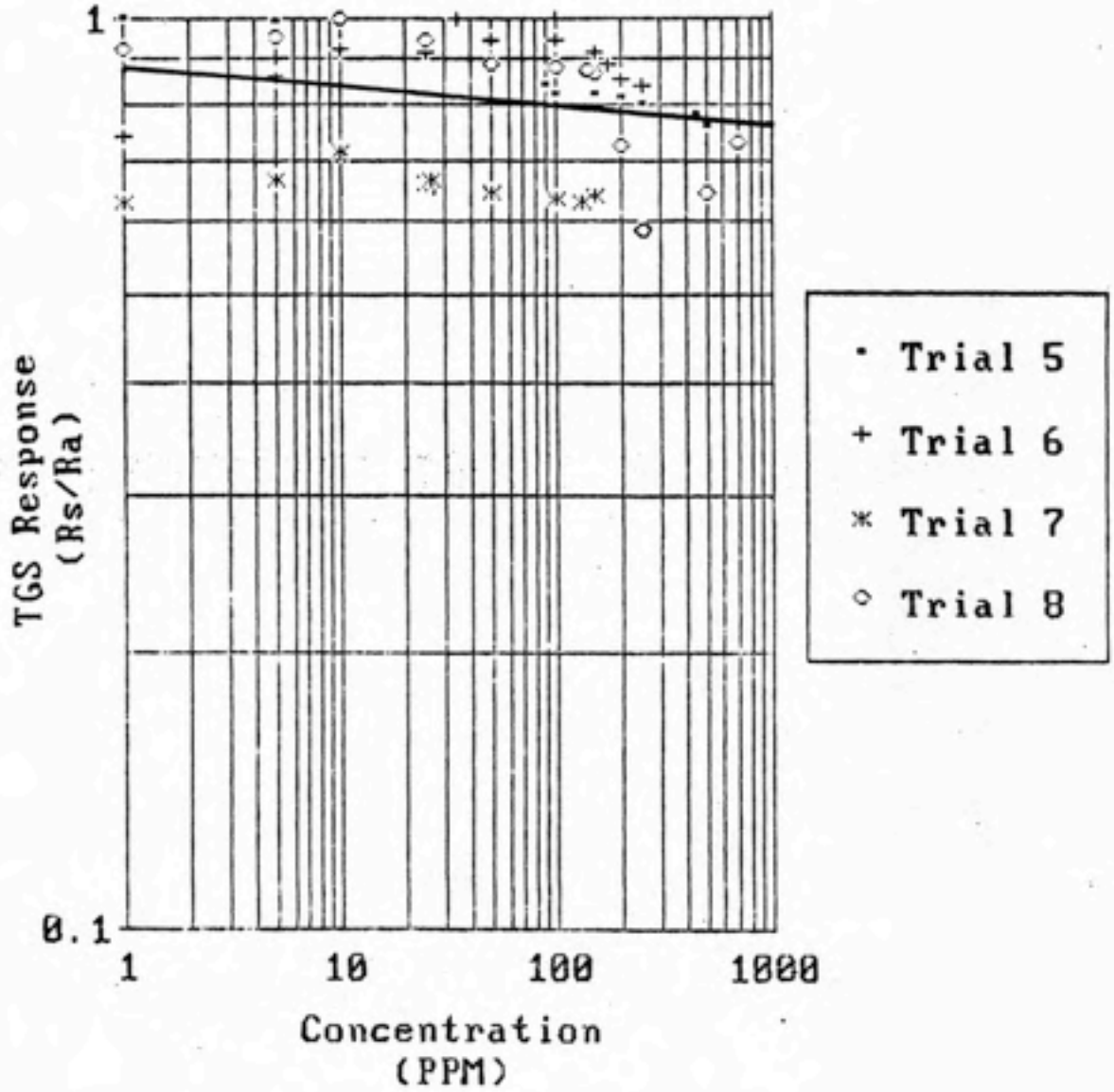

TGS Toluene Calibration Curve
(Gartland's Data)

Figure 18

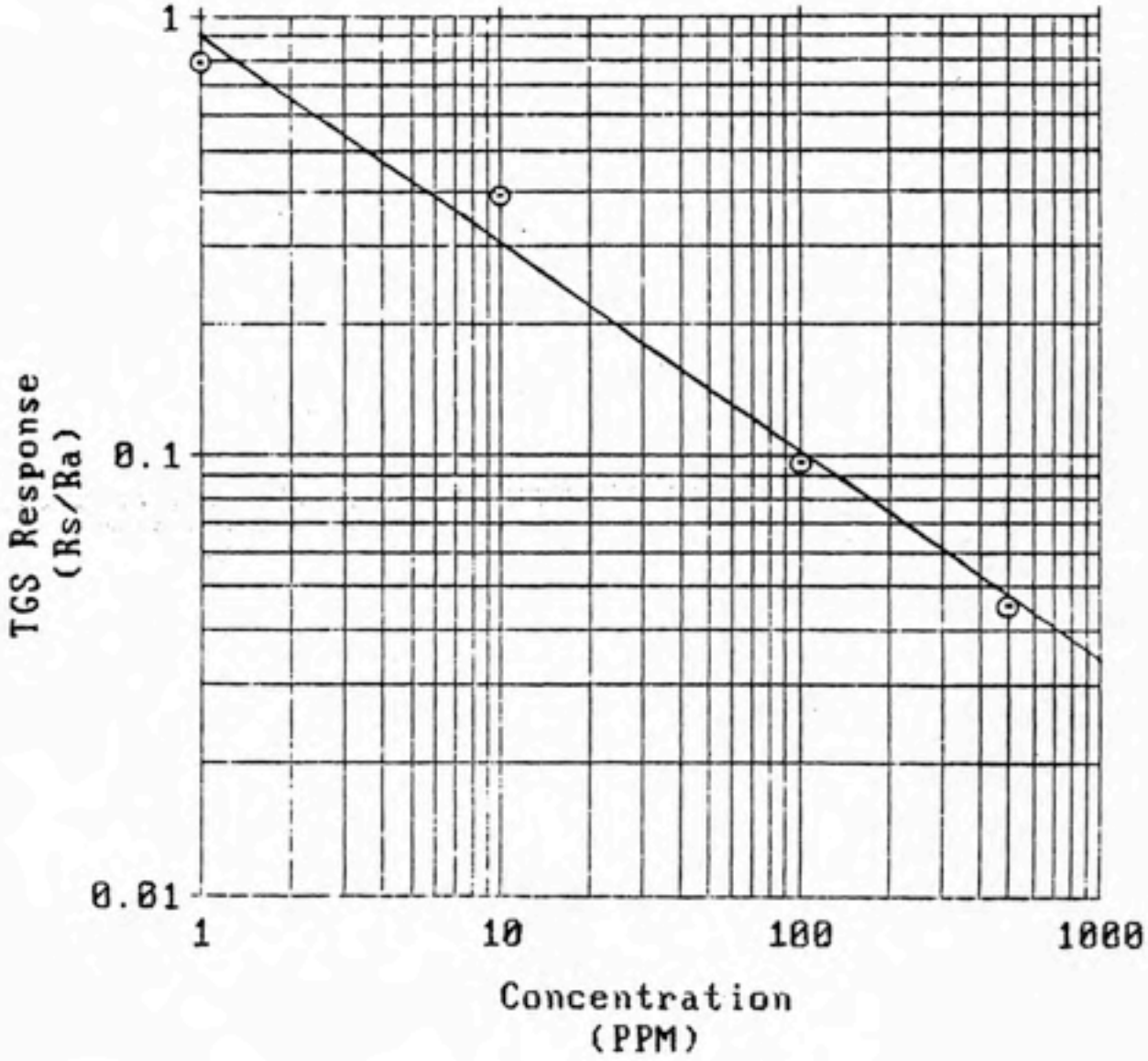

TGS Toluene Calibration Curve
(Bratt's Data)

Figure 19

31 makes it evident that there has been a large loss in sensitivity to toluene between Bratt's study and this current study. The TGS 812 response to toluene in the current study is also more erratic, although a noticeable increase in sensitivity occurs above 100 ppm toluene in Figure 18.

This erratic response was also present in the preliminary evaluation of carbon tetrachloride. Bratt's tests of TGS 812 response to carbon tetrachloride showed a very small sensitivity (shallow slope on a response curve). The overall response sensitivity of the sensor seems to have deteriorated since Bratt's study. It is therefore not surprising that carbon tetrachloride response could not be detected even at high concentrations.

2. TGS 812 binary mixture response

Response of the TGS 812 to binary mixtures of acetone and toluene was also evaluated. Selected response values are presented in Table 6. The TGS response values for the selected acetone concentrations are presented in the columns on the left along with the complementary toluene concentration present at that same point in the test. This same procedure is used in presenting the toluene data in the columns on the right along with the complementary acetone date.

Acetone data for Trial 9 is absent below 450 ppm. This is due to the quick breakthrough time of acetone. Trial 9 was the first binary test and the procedure used was found to be inadequate. The sampling system was adjusted in this trial to measure challenge concentration first. When the challenge concentration reading had stabilized the sampling system was re-adjusted to measure breakthrough concentration.

TABLE 6

TGS 812 Response (Rs/Ra) in Binary Solvent Tests

	Trial 9		Trial 10		Trial 11		Trial 12	
	Acetone	Toluene	Acetone	Toluene	Acetone	Toluene	Acetone	Toluene
Challenge Concentration (ppm)	546.10	541.50	1179.00	746.80	573.7	364.2	232.8	290.7
Acetone Concentration (ppm)	(*)---	462.40	1.00	67.84	1.00	94.40	1.00	72.80
Toluene Concentration (ppm)	---	1.00	0	1.00	0	1.00	0	1.00
TGS Response (Rs/Ra)	---	0.385	0.927	0.483	0.977	0.370	1.000	0.336
Acetone Concentration (ppm)	---	664.00	10.00	961.60	10.00	648.00	10.00	276.80
Toluene Concentration (ppm)	---	10.00	0.20	10.00	0	10.00	0	10.00
TGS Response (Rs/Ra)	---	0.367	0.710	0.260	0.633	0.237	0.813	0.172

(*) Sampling system was set to record challenge concentration. Was not returned to downstream until after 50% acetone breakthrough.

(Continued on next page)

TABLE 6 (Continued)
TGS 812 Response (Rs/Ra) in Binary Solvent Tests

	Trial 9		Trial 10		Trial 11		Trial 12	
	Acetone	Toluene	Acetone	Toluene	Acetone	Toluene	Acetone	Toluene
Acetone Concentration (ppm)	---	784.80	50.00	1600.00	50.00	702.40	50.00	287.20
Toluene Concentration (ppm)	---	50.00	0.60	50.00	0.40	50.00	0.40	50.00
TGS Response (Rs/Ra)	---	0.360	0.531	0.248	0.503	0.237	0.448	0.167
Acetone Concentration (ppm)	---	---	100.00	1600.00	100.00	677.60	100.00	273.60
Toluene Concentration (ppm)	---	---	1.00	100.00	1.20	100.00	1.76	100.00
TGS Response (Rs/Ra)	---	---	0.449	0.248	0.359	0.232	0.286	0.171
Acetone Concentration (ppm)	---	---	150.00	1566.00	150.00	636.00	150.00	---
Toluene Concentration (ppm)	---	---	1.92	150.00	1.36	150.00	2.20	---
TGS Response (Rs/Ra)	---	---	0.382	0.248	0.326	0.232	0.227	---
Acetone Concentration (ppm)	---	---	200.00	---	200.00	605.60	200.00	---
Toluene Concentration (ppm)	---	---	2.08	---	1.92	200.00	3.32	---
TGS Response (Rs/Ra)	---	---	0.358	---	0.295	0.231	0.198	---

It was discovered at this time that the acetone reading was already past the 50% breakthrough. Based on these results, all following binary tests were performed with the breakthrough readings measured first as described in the procedure section of this paper.

In evaluating the TGS 812 binary vapor response several patterns of results should first be discussed. As has been mentioned, the response to acetone was stronger and more definitive than to toluene. The response of the sensor to these solvents was also affected in this study by the ability of the solvent to be adsorbed on the charcoal bed. Acetone was less strongly adsorbed and was thus always the first solvent to breakthrough. This breakthrough pattern meant that it was the affect of toluene breakthrough on the already occurring acetone response which should be investigated.

To evaluate the binary response, a linear regression was performed of the TGS response (R_s/R_a) versus the natural logarithms of acetone concentration (lnA) and toluene concentration (lnT):

$$TGS = 0.611 - (0.043)(lnA) - (0.027)(lnT) \quad (32)$$

A correlation coefficient (R^2) of 0.60 was obtained. This was a slightly better fit than found for a linear regression using ln TGS (R^2=0.55). It should be noted that response values which occurred before toluene began breakthrough were not included in this regression since ln (0) is not a real number. A plot of Eq. 32 is presented in Figure 20. Examination of both Figure 20 and Eq. 32 shows that acetone has a stronger effect on response of the TGS 812 than toluene when an equal mixture of the two contaminants is present.

The combination of the rapid breakthrough of acetone and the relatively poor response of the sensor to toluene makes evaluation of

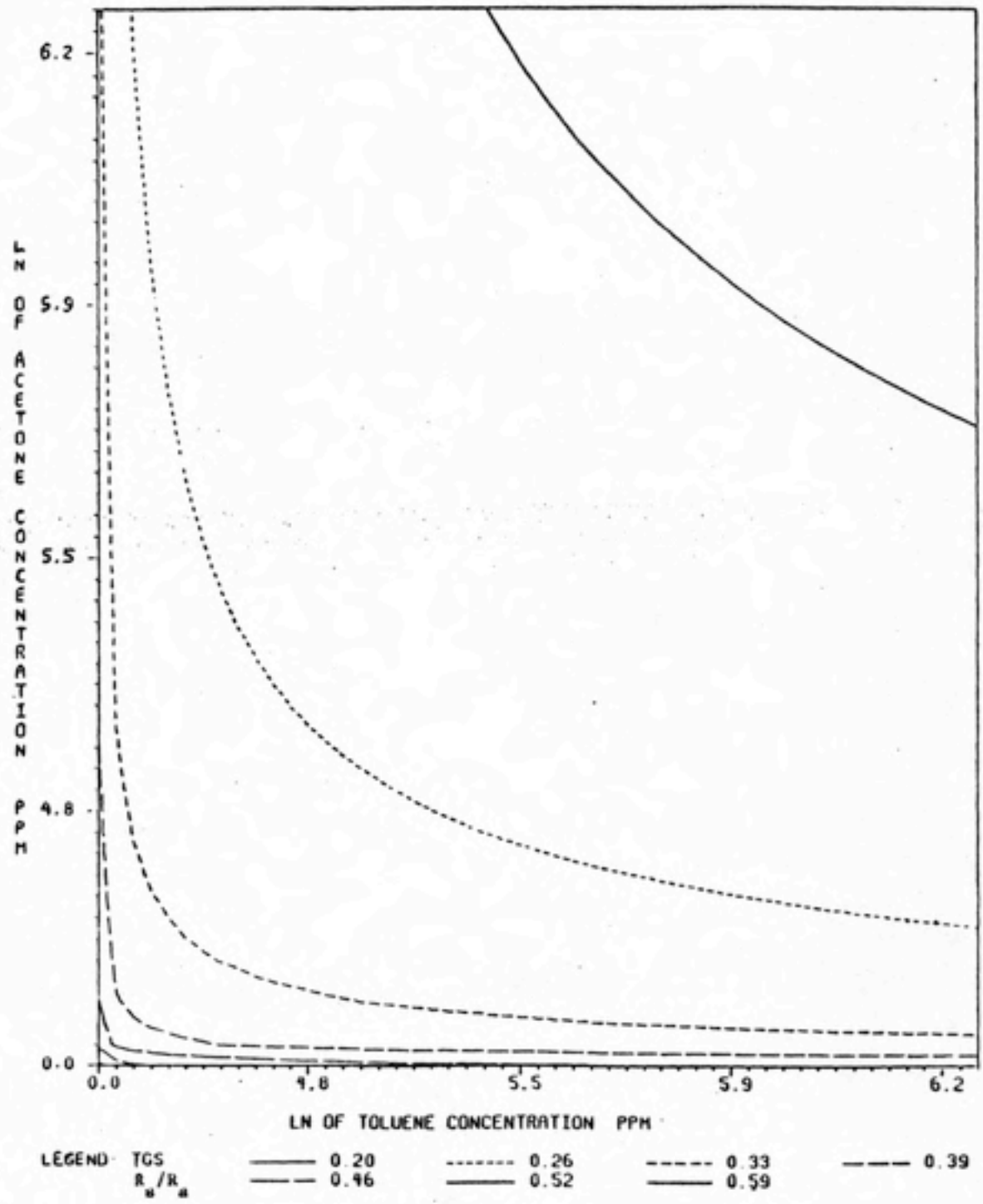

Figure 20. TGS 812 Response to Acetone/Toluene Binary Mixtures

the binary solvent response difficult. Examination of Table 6 shows that the 10% breakthrough points for acetone occur in each trial at times when toluene values were very low (less than 10 ppm).

Based on the single tests of toluene vapor, it is not expected that these low toluene values would affect the ability of the sensor to set off the alarm at the pre-set 10% acetone breakthrough. This statement must be tempered by the consideration of the apparently large drop in sensitivity found when comparing the single solvent tests results found in this study with those of Bratt (6). It is possible that the toluene would have had an affect on the sensor response to acetone breakthrough if the sensor was as sensitive as in Bratt's study.

3. TGS 812 fresh air resistance

Another factor to be considered when evaluating the sensor response to contaminants is the stability of its fresh air resistance. Examination of Figure 21 shows that this resistance was relatively constant for the single solvent tests (Trials 1 - 8), but begins to rise steeply during the binary tests. This rise suggests either a fault in the sensor or the effect of an uncontrolled environmental factor. Table 7 contains the fresh air resistance value, room temperature and relative humidity readings for each trail. Both of the environmental factors increased during the last three trials, but the effect these changes would have are the opposite of those observed. Examination of Figure 5 and Eq. 7 shows that an increase in either factor should cause a drop in resistance rather than a rise.

There are two other possible causes for this increasing

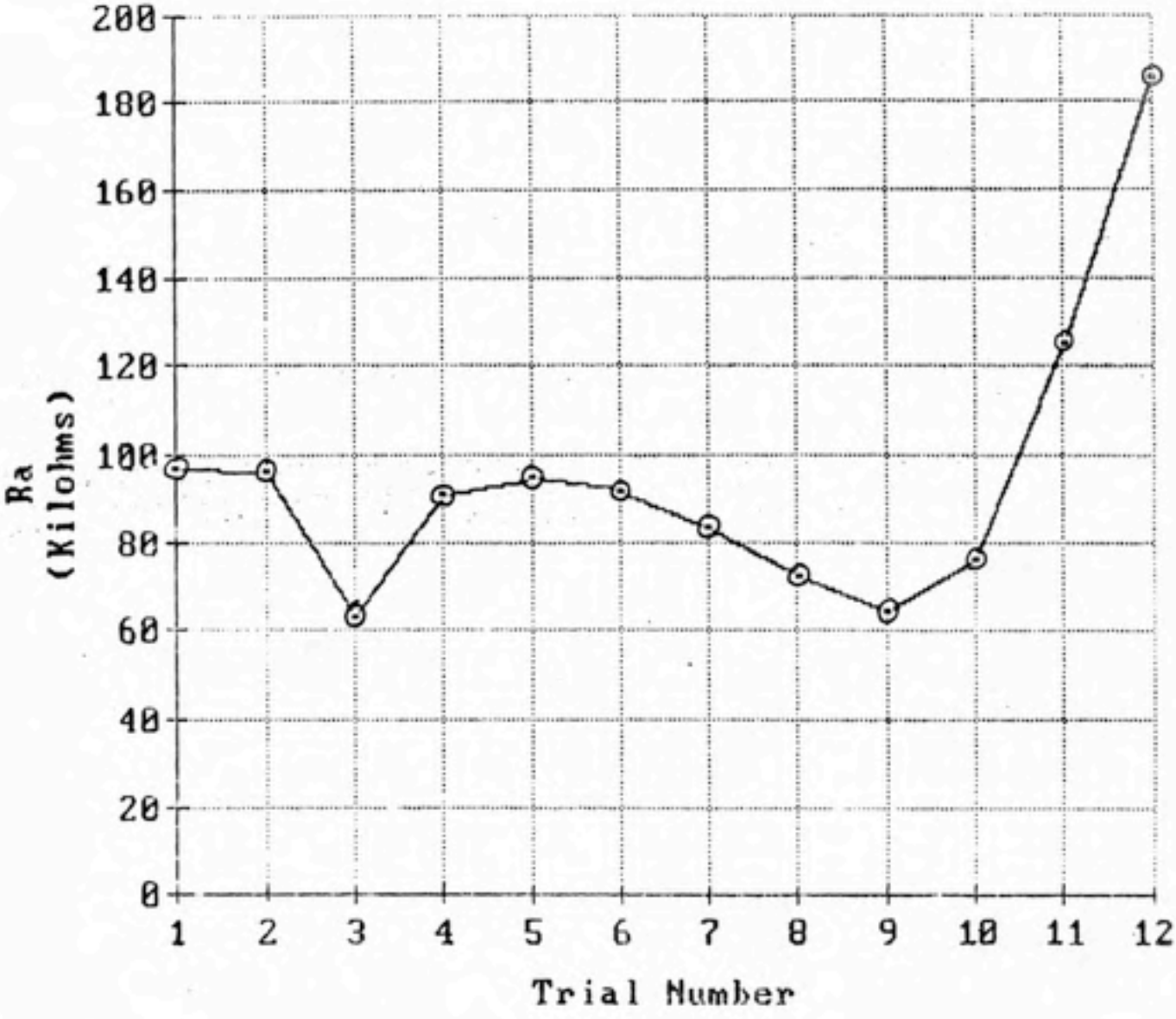

Variation in TGS
Resistance in Air

Figure 21

TABLE 7

TGS 812 Fresh Air Resistance (Ra) and Environmental Conditions

Trial Number	Ra (Kilohms)	Room Temperature (°C)	Relative Humidity (%)
1	97.097	22.3	---
2	95.957	22.0	44.0
3	63.235	21.8	48.5
4	91.220	22.5	48.0
5	94.842	23.0	48.0
6	91.633	24.0	47.0
7	83.084	22.6	50.0
8	72.314	22.3	65.0
9	64.107	23.2	---
10	75.862	23.4	47.0
11	124.595	23.5	54.0
12	185.294	23.7	60.0

resistance. One possibility is that the house air supply may have become contaminated with an oxidizing gas which would cause an increase in the sensor resistance in a manner similar to that described for oxygen. The other and more likely cause for the resistance increase is failure of the sensor. It has already been established that sensor sensitivity has decreased to a large extent when compared with Bratt's study (6). The fact that the sensor resistance rose rather steadily when environmental conditions should be causing a drop in resistance further supports this theory.

This fresh air resistance change and the relatively poor fit (R^2 = 0.60) of Eq. 32 make it difficult to provide a clear cut conclusion based on the binary tests. It does appear that the ability of acetone to reach breakthrough quicker and to react more strongly with the sensor suggests that this sensor could possibly be used in breakthrough monitoring for ventilation systems where these two solvents are in use. No predictions for other solvents can be made based on the binary test results in this study. Further research is needed.

B. CHARCOAL BED EVALUATION

The Fisher activated charcoal was characterized using methods described by Bartosh (4). The results of these characterization procedures are presented in Appendix C.

The adsorption capacity at the 10% breakthrough point was calculated for all except the last of the single vapor trials. The breakthrough curve for Trial 8 could not be weighed as required in

these calculations. The gain scale had to be reduced during this trial, thus changing the proportionality between curve size and the concentration of toluene present. The adsorption capacity and other charcoal bed adsorption parameters for each single solvent trial are presented in Table 8. It is clear from the lower calculated adsorption capacities that acetone is less strongly adsorbed on the charcoal than the toluene. It would be expected that acetone will thus have a shorter time to 10% breakthrough than toluene for the same concentration of each solvent.

The actual and predicted breakthrough results are presented in Table 9. Nelson and Correia's (31) equation, Eq. 29, consistently overestimated time for acetone. Equation 29 also underestimated all the toluene 10% breakthrough times except for that of Trial 8, which it overestimated by less than 5%.

Equation 31 was found to be quite accurate for prediction of 10% breakthrough times as compared to Eq. 29. This is not surprising considering the sources of the adsorption capacity values for each equation. Eq. 29 utilizes a theoretical adsorption capacity value calculated from a range of solvents within a chemical family. Eq. 31 utilizes the estimate of adsorption capacity found in Table 8 which is a crude value, but more directly associated with the solvent of interest.

Both acetone and toluene 10% breakthrough times (t_B) fit well to Eq. 30 describing a power slope relation to challenge concentration (C) (ie. $t_B = aC^b$). Acetone had a power coefficient (b) of -0.515 and a correlation coefficient (R^2) of 0.998. Toluene had a power coefficient of -0.830 and a correlation coefficient of 0.976. The 10%

TABLE 8

Charcoal Bed Adsorption Parameters for the Single Solvent Tests

Trial No.	C	M	Ads.	Q	PD	Atm.	RT	RH
1-A	119.3	49.403	0.031	69.58	11.2	753.8	22.3	---
2-A	617.2	49.400	0.075	69.86	11.5	755.8	22.0	44.0
3-A	1062.7	49.402	0.093	70.17	11.6	759.1	21.8	48.5
4-A	1110.1	49.454	0.098	70.21	11.1	757.1	22.5	48.0
5-T	904.1	49.395	0.437	69.18	10.2	755.2	23.0	48.0
6-T	347.7	49.404	0.363	68.08	10.8	751.6	24.0	47.0
7-T	263.8	49.405	0.293	69.82	11.3	756.6	22.6	50.0
8-T	1386.6	49.407	---	69.08	10.1	749.4	22.3	65.0

Abbreviations

A = Acetone
T = Toluene
C = Challenge concentration in ppm.
M = Mass of charcoal in gm.
Ads = Adsorption capacity in gm solvent/gm charcoal.
Q = Air flow rate in L/min.
PD = Pressure drop across charcoal bed in mm of water.
Atm = Atmosphere pressure in mm of mercury.
RT = Room temperature in ^{o}C.
RH = Percent relative humidity.

TABLE 9

Single Vapor Breakthrough Results

Trial No.	C	Eq.29	%Dev.	Eq.31	%Dev.	T10%	T50%
1-A	119.3	242.90	+65.41	77.65	-8.19	84.01	146.01
2-A	617.2	80.52	+53.42	36.01	-4.17	37.51	75.11
3-A	1062.7	55.53	+51.83	25.69	-2.26	26.75	54.91
4-A	1110.1	54.23	+50.30	26.06	-3.42	26.95	51.55
5-T	904.1	78.07	-20.32	91.54	-2.61	93.93	129.05
6-T	347.7	151.27	-39.23	202.60	-3.95	210.61	248.61
7-T	263.8	175.31	-24.31	207.79	-4.88	217.93	274.73
8-T	1386.6	59.12	+ 4.72	----	----	56.33	95.93

Abbreviations

A = Acetone
T = Toluene
C = Challenge concentration in ppm.
Eq.29= 10% breakthrough time in min predicted by Equation 29.
Eq.31= 10% breakthrough time in min predicted by Equation 31.
%Dev.= Percent deviation of calculated from measured 10% breakthrough time.
T10% = Measured 10% breakthrough time in min.
T50% = Measured 50% breakthrough time in min.

breakthrough times are plotted against challenge concentration for each solvent in Figure 22.

Typical breakthrough curves for acetone, toluene and a binary mixture of them both are presented in Figures 23, 24 and 25, respectively. Table 10 contains the charcoal bed adsorption parameters for the binary tests. Table 11 contains the breakthrough times for the individual solvents in each binary test. An examination of Table 11 and Figure 25 shows that the same general pattern was followed for breakthrough as with the single solvent tests. Acetone breakthrough was much faster than that of toluene.

Comparison of Tables 9 and 11 brings to light another pattern for these binary tests. The acetone achieves 10% and 50% breakthrough in much shorter time. This can also be seen when comparing Figures 23, 24 and 25 since the concentration of each single solvent is similar to the concentration of that solvent in the binary mixture. These figures correspond to Trials 2, 6 and 11, respectively. Comparison of the acetone 10% breakthrough times for Trials 2 and 11 shows that the acetone is achieving breakthrough almost 25% faster than would be expected with a single vapor. This same pattern was noted by Bartosh (4) in his study on binary solvent effects on respirator cartridge breakthrough.

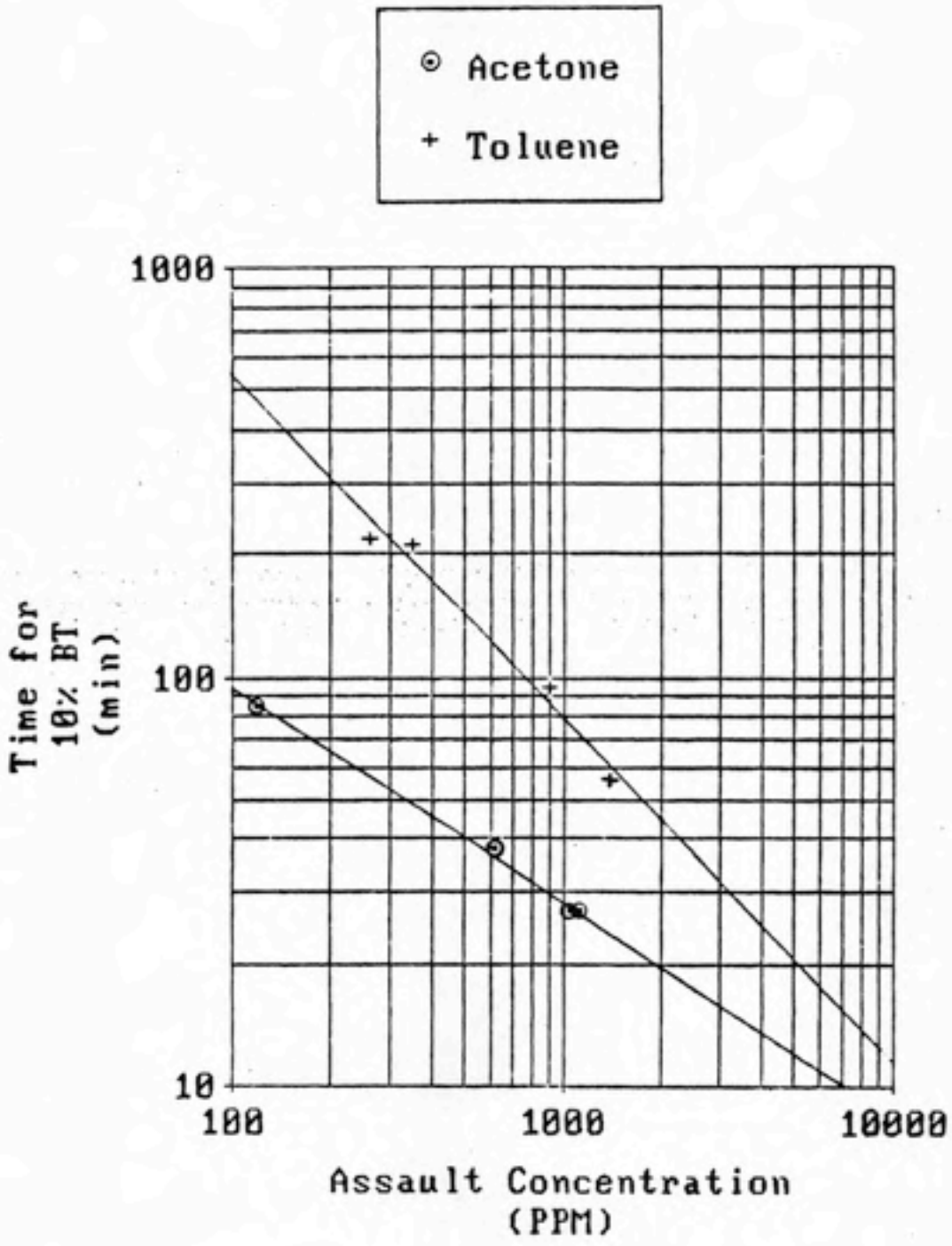

10% Breakthrough Times
vs
Assault Concentration

Figure 22

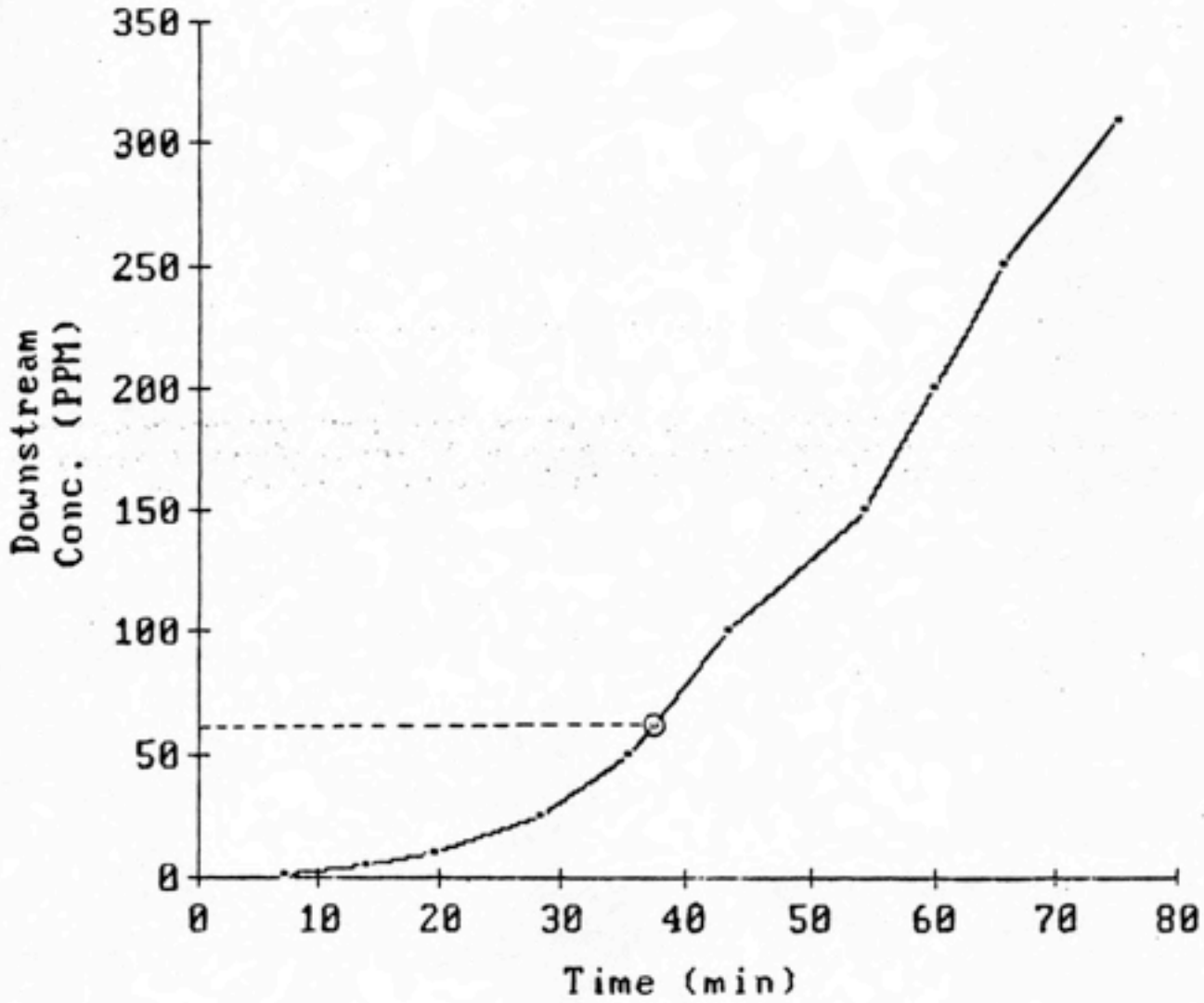

Breakthrough Curve for Acetone
(Trial # 2)
Assault Concentration =617.2
PPM

Figure 23

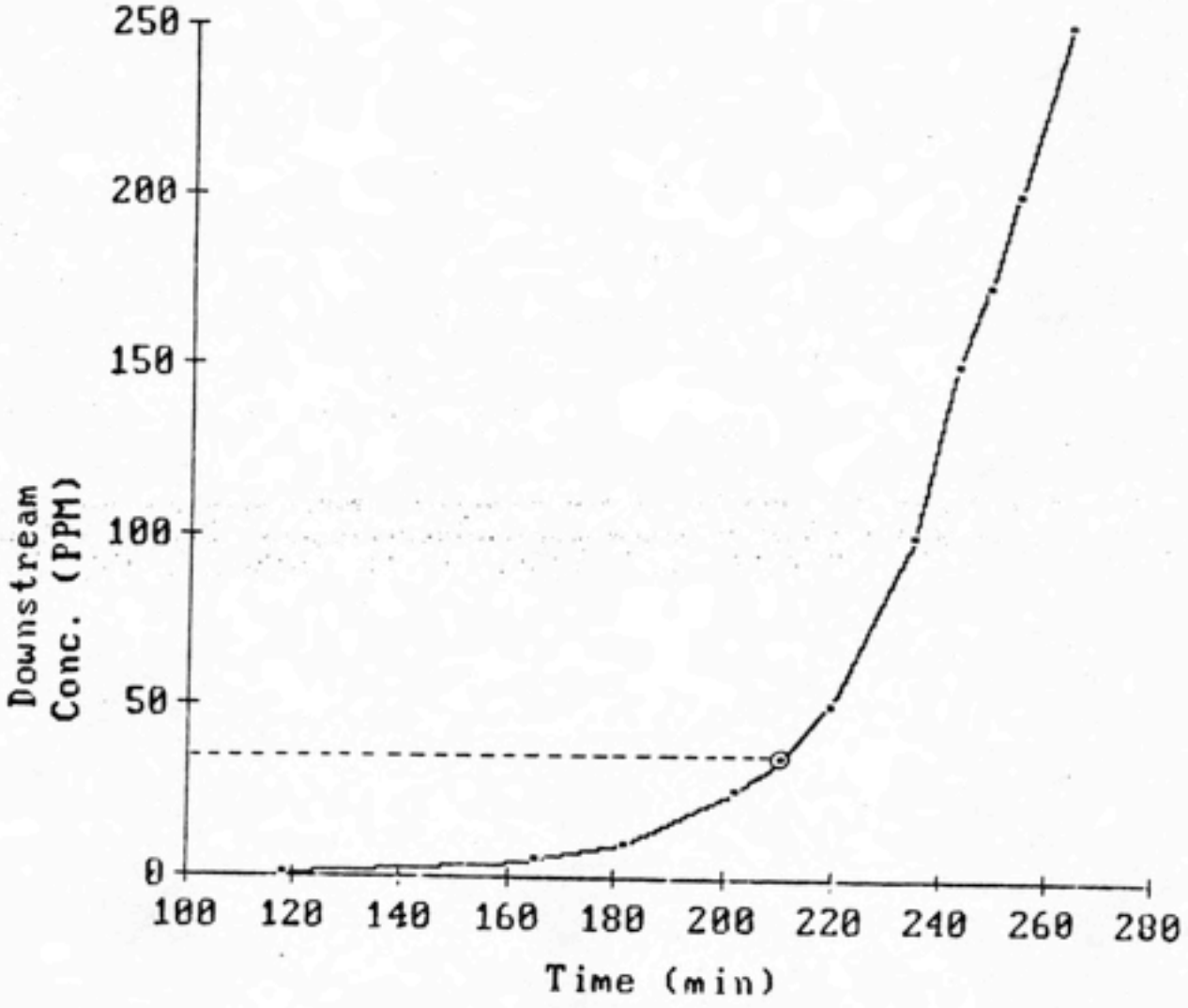

Breakthrough Curve for Toluene
(Trial # 6)
Assault Concentration =347.7
PPM

Figure 24

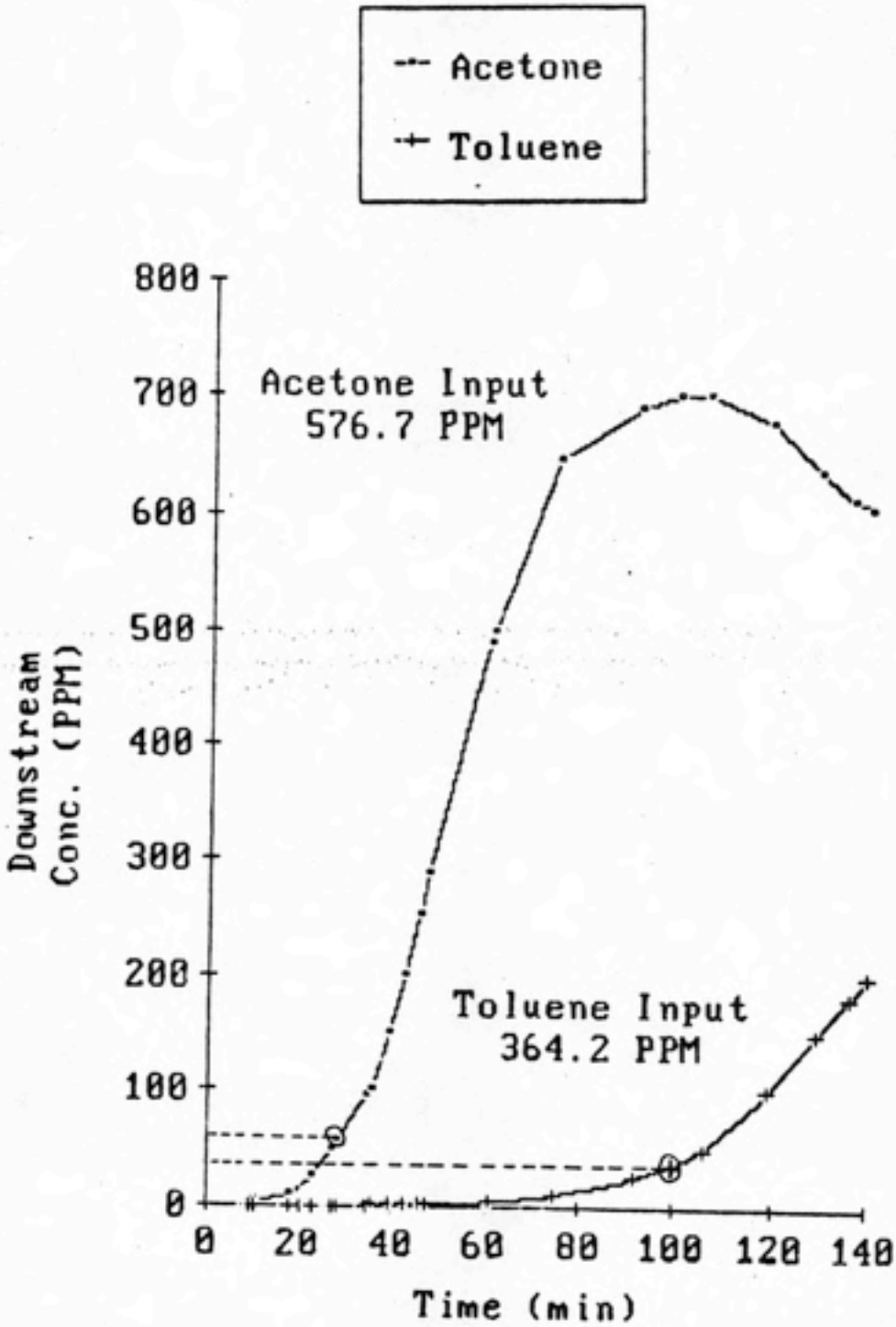

Breakthrough Curves
for Trial # 11

Figure 25

TABLE 10

Charcoal Bed Adsorption Parameters for Binary Vapor Tests

Trial No.	CA	CT	M	QT	PD	Atm	RT	RH
9	546.1	541.5	49.401	70.42	11.2	759.7	23.2	----
10	1179.0	746.8	49.399	70.83	10.5	764.8	23.4	47.0
11	576.7	364.2	49.407	72.02	9.7	756.6	23.5	54.0
12	232.8	290.7	49.401	69.49	9.4	755.1	23.7	60.0

Abbreviations

CA = Challenge concentration of acetone in ppm.
CT = Challenge concentration of toluene in ppm.
M = Mass of charcoal in gm.
QT = Total flow rate passing through the bed in L/min.
PD = Pressure drop across charcoal bed in mm of water.
Atm = Atmospheric pressure in mm of mercury.
RT = Room temperature in °C.
RH = Percent relative humidity.

TABLE 11

Binary Solvent Breakthrough Results

	Acetone			Toluene		
Trial No.	C	T10%	T50%	C	T10%	T50%
9	546.1	----	----	541.5	76.91	----
10	1179.0	15.51	25.77	746.8	55.21	----
11	576.7	28.05	47.43	364.2	99.93	135.93
12	232.8	41.97	71.99	290.7	184.37	----

Abbreviations

C = Challenge concentration in ppm.

T10% = 10% breakthrough time in min.

T50% = 50% breakthrough time in min.

V. CONCLUSIONS

The stated objective of this study was to evaluate the effect of binary solvent mixtures on the ability of an organic vapor detector, the TGS 812, to be utilized as a breakthrough monitor for a charcoal bed filter system.

When consideration is given to the relatively rapid breakthrough times and the greater sensitivity of the TGS 812 for acetone, it would appear that the sensor can be used as a breakthrough detector when air containing mixtures of acetone and toluene must be purified. This statement must be tempered with the fact that the sensor had shown a large sensitivity decrease to the solvents used here when compared with a previous study of single solvent response with the exact same sensor (6). Comparison of the single vapor tests with the binary vapor tests showed that acetone 10% breakthrough in the binary tests occurred at points where toluene concentrations were sufficiently low that they probably could not contribute appreciably to a change in the sensor response. This may not hold true with new sensors working at peak efficiencies. Time considerations did not allow further testing with new sensors to test this idea.

The results of this study suggest that the sensor can be used as an acetone-toluene binary mixture breakthrough detector. Extrapolation to other mixtures is difficult, although it is probable that this sensor could be used in any system where acetone was predicted to

breakthrough more rapidly than the other component. Such predictions are beyond the scope of this current project.

Charcoal bed breakthrough response occurred as predicted by carbon theory. The more volatile acetone was less strongly adsorbed in the bed and thus achieved breakthrough more rapidly in both the single and binary tests. Both acetone and toluene achieved good fit in the single tests to the power relationship between 10% breakthrough time (t_B) and challenge concentration (C) described by Nelson and Correia (31): $t_B = aC^b$.

VI. RECOMMENDATIONS

It is clear from comparison of the results achieved here for single vapor tests with those of Bratt (6) that the TGS 812 sensor is capable of greater sensitivities than were achieved here. It is thus clear that further testing is needed.

One possible study to be performed would utilize a bank of sensors as Bratt (6) did in his calibration tests. This bank of sensors could be placed in a duct system downstream of an actual charcoal bed while known concentrations of binary solvent mixtures are passed through the bed. The bank of sensors would help eliminate problems such as those encountered in this study where possible failure of a single sensor can make results difficult to interpret.

The electronic circuitry associated with the sensor could be redesigned to allow adjustment of the heater voltage in the sensor to achieve greater sensitivity by approaching the optimum response temperature of one of the solvents in a pair. Tuma and Clifford (43) have suggested using a microcomputer system to control a bank of sensors in this way.

A recent study by Jonas, et al, (20) presented a new method for prediction of activated carbon performance for binary vapor mixtures. The adsorption capacity for each individual component can be calculated by this method and 10% breakthrough predictions made utilizing Eq. 31. A procedure based on these predictions would help select further pairings of solvents for binary testing of the sensor.

REFERENCES

1. Abrams, D. S., "An Evaluation of the Effectiveness of a Recirculating Laboratory Hood", A report submitted to the Faculty of the University of North Carolina at Chapel Hill in partial fulfillment of the requirements for the degree of Master of Science in Public Health in the Department of Environmental Sciences and Engineering (1983).
2. Advani, G. N. and Nanis, L., "Effects of Humidity on Hydrogen Sulfide Detection by SnO_2 Solid State Gas Sensors", Sensors and Actuators, Vol. 2, pp. 201-206, (1981/1982).
3. American Conference of Governmental Industrial Hygienists, TLV's: Threshold Limit Values for Chemical Substances and Physical Agents in the Work Environment with Intended Changes for 1983-84, Cincinnati, OH (1983).
4. Bartosh, E. T., Jr., " Influences of Binary Mixtures on Organic Vapor Respirator Cartridge Service Life", A report submitted to the Faculty of The University of North Carolina at Chapel Hill in partial fulfillment of the requirements for the degree of Master of Science in Environmental Engineering in the Department of Environmental Sciences and Engineering (1979).
5. Boyle, J. F. and Jones, K. A., "The Effects of CO, Water Vapor and Surface Temperature on the Conductivity of a SnO_2 Gas Sensor", Journal of Electronic Materials, Vol. 6, pp. 717-733, (1977).

6. Bratt, G. M., "Development of an Electronic End of Life Organic Vapor Respirator Cartridge Indicator", A report submitted to the Faculty of the University of North Carolina at Chapel Hill in partial fulfillment of the requirements for the degree of Master of Science in Environmental Engineering in the Department of Environmental Sciences and Engineering (1980).

7. Brown, V. R. and Kroes, D. J., "Metallic Oxide Semiconductor Sensors for Combustible Gas and Vapor Monitoring", Analysis Instrumentation, Vol. 15, pp. 83-86, (1977).

8. Charcoal Service Corporation, High Efficiency Gas Adsorbers (HEGA), Bulletin No. 283A, (Company Brochure).

9. Clifford, P. K. and Tuma, D. T., "Characteristics of Semiconductor Gas Sensors: I. Steady State Gas Response", Sensors and Actuators, Vol. 3, pp. 233-254, (1982/1983).

10. Clifford, P. K. and Tuma, D. T., "Characteristics of Semiconductor Gas Sensors: II. Transient Response to Temperature Change", Sensors and Actuators, Vol. 3, pp. 255-281, (1982/1983).

11. Figaro USA, Inc., Figaro Gas Sensor: TGS 812, Figaro USA, Inc., Wilmette, IL, (Dec., 1983).

12. Figaro USA, Inc., Figaro TGS Gas Sensor: General Catalog, Figaro USA, Inc., 322 Wilshire Dr., Wilmette, IL 60091, (Dec., 1983).

13. Figaro USA Inc., Semiconductor Gas Sensor, Figaro USA, Inc., Wilmette, IL, (Dec., 1983).

14. Firth, J. G., Jones, A. and Jones, T. A., "Solid State Detectors for Carbon Monoxide", Annals of Occupational Hygiene, Vol. 18, pp. 63-68, (1975).

15. Foxboro Analytical, 1982 OSHA Concentration Limits for Gases Incorporating Infrared Analytical Data for Compliance Testing and Other Applications, Wall Chart, Foxboro Analytical, (1981).

16. Grubner, O. and Burgess, W. A., "Calculation of Adsorption Breakthrough Curves in Air Cleaning and Sampling Devices", Environmental Science and Technology, Vol. 15, pp. 1346-1351, (1981).

17. Grubner, O. and Burgess, W. A., "Simplified Description of Adsorption Breakthrough Curves in Air Cleaning and Sampling Devices", American Industrial Hygiene Association Journal, Vol. 40, pp. 169-179, (1979).

18. Heiland, G., "Homogenous Semiconducting Gas Sensors", Sensors and Actuators, Vol. 2, pp. 343-361, (1982).

19. Ihokura, K., "Tin Oxide Gas Sensor for Deoxidizing Gas", New Materials & New Processes, Vol. 1, pp. 43-50, (1981).

20. Jonas, L. A., Sansone, E. B. and Farris, T. S., "Prediction of Activated Carbon Performance for Binary Vapor Mixtures", American Industrial Hygiene Association Journal, Vol. 44, pp. 716-719, (1983).

21. Jones, T. A., "Towards a Robust Monitor for Detecting Toxic Gases", Sensor Review, Vol. 1, pp. 14-19, (1982).

22. Kennedy, E. R., Preliminary Evaluation of a Prototype Organic Vapor Respirator End of Service Life Indicator, National Institute for Occupational Safety and Health, Cincinnati, OH, (Feb., 1980).

23. Lalauze, R. and Pijolat, C., "A New Approach to Selective Detection of Gas by an SnO_2 Solid-State Sensor", Sensors and Actuators, Vol. 5, pp. 55-63, (1984).

24. Linch, A. L., Evaluation of Ambient Air Quality by Personnel Monitoring: Volume I: Gases and Vapors, 2nd Edition, CRC Press, Inc., Boca Raton, FL, 1981, pp. 28-32.

25. Loschiavo, J., "Quantitative Respirator Fit Testing Using Ethanol as the Tracer", A report submitted to the Faculty of the University of North Carolina at Chapel Hill in partial fulfillment of the requirements for the degree of Master of Science in Public Health in the Department of Environmental Sciences and Engineering, (1979).

26. Many, A., "Relation between Physical and Chemical Processes on Semiconductor Surfaces", CRC Critical Reviews in Solid State Sciences, Vol. 4, pp. 515-539, (1974).

27. Michaelis, T. B., Techniques to Detect Failure in Carbon Adsorption Systems, U. S. Environmental Protection Agency, Washington, D. C., EPA 340/1-80-011, (April, 1980).

28. Morrison, S. R., "Semiconductor Gas Sensors", Sensors and Actuators, Vol. 2, pp. 329-341, (1982).

29. National Institute for Occupational Safety and Health, Development of a Prototype Service-Life Indicator for Organic Vapor Respirators, National Institute for Occupational Safety and Health, Cincinnati, OH, DHEW (NIOSH) Publication No. 78-170, (Aug. 1978).

30. Nelson, G. O., Controlled Test Atmospheres: Principles and Techniques, Ann Arbor Science Publishers, Inc., Michigan, 1971, pp. 217-219.

31. Nelson, G. O. and Correia, A. N., "Respirator Cartridge Efficiency Studies: VIII. Summary and Conclusions", American Industrial Hygiene Association Journal, Vol. 37, pp. 514-525, (1976).

32. Nelson, G. O. and Harder, C. A., "Respirator Cartridge Efficiency Studies: V. Effect of Solvent Vapor", American Industrial Hygiene Association Journal, Vol. 35, pp. 391-410, (1974).

33. Nitta, M. and Haradome, M., "Thick Film CO Gas Sensors", IEEE Transactions of Electron Devices, Vol. ED-26, pp. 247-249, (1979).

34. Nitta, M., Kanefusa, S. and Haradome, M., "Propane Gas Detector Using S_nO_2 Doped with Nb, V, Ti or Mo", Journal of the Electrochemical Society: Solid-State Science and Technology, Vol. 125, pp. 1676-1679, (1978).

35. Occupational Safety and Health Administration, Title 29. Code of Federal Regulations. Part 1910, 1000, "Air Contaminants", OSHA 2206 General Industry. Revised June, 1981.

36. Oyabu, T., "Sensing Characteristics of S_nO_2 Thin Film Gas Sensors", Journal of Applied Physics, Vol. 53, pp. 2785-2787, (1982).

37. Oyabu, T., Osawa, T. and Kurobe, T., "Sensing Charateristics of Tin Oxide Thick Film Gas Sensor", Journal of Applied Physics, Vol. 53, pp. 7125-7130, (1982).

38. Reist, P. C., Personal Communication, March, 1983.

39. Reist, P. C. and Cole, H. M., "A Simple Procedure for the Routine Testing of Respirator Sorbents", American Industrial Hygiene Association Journal, Vol. 33, pp. 523-525, (1972).

40. Seiyama, T. and Kagawa, S., "Study on a Detector for Gaseous Components Using Semiconductrive Thin Films", Analytical Chemistry, Vol. 38, pp. 1069-1073, (1966).

41. Seiyama, T., Kato, A., Fujiishi, K. and Nagatani, M., "A New Detector for Gaseous Components Using Semiconductive Thin Films", Analytical Chemistry, Vol. 34, pp. 1502-1503, (1962).

42. Stetter, J. R., "A Surface Chemical View of Gas Detection", Journal of Colloid and Interface Science, Vol. 65, pp. 432-443, (1978).

43. Tuma, D. T. and Clifford, P. K., "Microcomputer Control and Information Processing Technology for Semiconductor Gas Sensors", in Proceedings of the Symposium on Development and Usage of Personal Monitoring for Exposure and Health Effect Studies, EPA 600/9-79-032, (June, 1979), pp. 191-206.

44. Turk, A., "Gaseous Air Cleaning to Maintain Tolerable Indoor Air Quality Limits", ASHRAE Transactions, Vol. 89 (IB), pp. 505-510, (1983).

45. Turk, A., Mark, H. and Mehlman, S., "Tracer Gas Nondestructive Testing of Activated Carbon Cells", Materials Research and Standards, Vol. 9, pp. 24-26, (1969).

46. Wainscott, D. T., "The Development of a New Method for Evaluating Chemical Permeation Through Industrial Gloves", A report submitted to the Faculty of the University of North Carolina at Chapel Hill in partial fulfillment of the requirements for the degree of Master of Science in Public Health in the Department of Environmental Sciences and Engineering, (1981).

47. Watson, J., "The Tin Oxide Gas Sensor and Its Applications", Sensors and Actuators, Vol. 5, pp. 29-42, (1984).

48. Watson, J. and Price, A., "Selectivity of Semiconductor Gas Sensors", Proceedings of the IEEE, Vol. 66, pp. 1670-1671, (1978).

49. Watson, J. and Tanner, D., "Applications of the Taguchi Gas Sensor to Alarms for Inflammable Gases", The Radio and Electronic Engineer, Vol. 44, pp. 85-91, (1974).

50. Weast, R. C. and Astle, M. J., eds., Chemical Rubber Company Handbook of Chemistry and Physics, 62nd Ed., CRC Press, Inc., Boca Raton, FL, (1981).

51. Windischmann, H. and Mark, P., "A Model for the Operation of a Thin-Film SnO_x Conductance - Modulation Carbon Monoxide Sensor", Journal of the Electrochemical Society: Solid-State Science and Technology, Vol. 126, pp. 627-633, (1979).

52. Yamazoe, N., Kurokawa, Y., and Seiyama, T., "Effects of Additives on Semiconductor Gas Sensors", Sensors and Actuators, Vol. 4, pp. 283-289, (1983).

APPENDIX A

CARBON ADSORPTION THEORY

CARBON ADSORPTION THEORY

The breakthrough response for a given organic vapor or gas in a charcoal bed is dependent on the strength of adsorption of the vapor. Adsorption is defined as a process in which a gas or liquid sorbate is attracted to a solid surface of a sorbent and is held in a gas-solid interface (17). These attractive forces can be categorized as either chemical or physical.

1. Chemical adsorption

Chemical adsorption involves sharing of electrons between the sorbate and sorbent to form a chemical bond. This bond formation often requires an activation energy input, occurring primarily at temperatures above 400 ^{o}F. This high heat requirement means that primarily physical adsorption should occur in this present study.

Physical adsorption on carbon involves relatively weak attractive forces known as Van der Walls forces. The sorbate must diffuse close to the carbon granule surface before these forces take effect. Carbon granule surfaces have many pores and micropores which can extend into the granule. Vapors which are trapped in these micropores tend to condense. It has been shown that a higher degree of pore filling will occur at high concentrations of relatively nonvolatile solvents as compared to low concentrations of volatile solvents (31).

2. Adsorption on activated carbon

Activated carbon is an electronically non-polar substance. It will adsorb most organic gases and vapors in preference to the more polar atmospheric moisture (24).

Chemicals can be divided into three categories in regards to their ability to be physically adsorbed on activated carbon (24). True gases, with critical temperatures less than -50 °C and boiling points less than -150 °C, are virtually non-adsorbable at normal temperatures. These gases include hydrogen, nitrogen, oxygen, carbon monoxide and methane. Low boiling vapors, having critical temperatures between 0 °C and 150 °C and boiling points between -100 °C and 0 °C are moderately adsorbable. These chemicals include ammonia, ethylene, formaldehyde, hydrogen chloride and hydrogen sulfide. Heavier vapors, having boiling points greater than 0 °C, will be readily adsorbed at normal temperatures. Chemicals falling into this category include most odorous organic and inorganic substances.

A number of studies have been made on charcoal cartridges to determine adsorption response trends. Some of the most extensive work in this area has been performed by Nelson, et al (31,32). They tested 121 different solvent vapors for sorptive capacity and breakthrough times in several types of respirator cartridges (32). Defining service life as the time to 10% breakthrough, it was found that the more volatile the chemical was, the shorter its service life. It was also found that a relative humidity greater than 65% would reduce the cartridge service, especially as the challenge concentration was reduced. It was also found that the service life was reduced 1 to 10% for each 10 °C increase in temperature. A predictive equation for

cartridge service life was developed by Nelson and Correia (31). They separated the 121 solvents tested into ten classes including acetates, alcohols, alkyl benzenes, ketones, etc. For each of these classes of compounds, plots were made of boiling point vs sorptive capacity and equations for best straight lines developed:

$$W_{ad} = a + bT \tag{28}$$

where W_{ad} is the theoretical adsorption capacity (gm/gm), T is the boiling point of the solvent of interest (°C), a is the intercept of the line and b the slope.

All of these plots were performed for 1000 ppm of each solvent. The a and b coefficients were selected for the solvent class of the solvent of interest and utilized along with the boiling point of that solvent to calculate the adsorption capacity, W_{ad}. This capacity was used to calculate the service life for that solvent:

$$t_{10\%} = \frac{(24.2)(10^6)(W_c)(W_{ad})}{(C)(MW)(Q)} \tag{29}$$

where $t_{10\%}$ is the 10% breakthrough time (min), W_c is the mass of charcoal in the test cartridge (gm), C is the challenge concentration (ppm), MW is the molecular weight of the solvent (gm/mole) and Q is the flow rate of the air stream through the cartridge (L/min).

It was also found that for a range of concentrations of a single solvent, the time to a given breakthrough percent, t_B, could be found from the expression:

$$t_B = aC^b \tag{30}$$

where C is the challenge concentration (ppm) and a and b are constants for given experimental conditions.

The average value for b at 10% breakthrough was -0.67 over a concentration range of 50 to 3000 ppm.

Abrams (1) evaluated several predictive equations for service life determination in his study of a recirculating fume hood. He found the best fit to be achieved utilizing an equation he had adapted from Grubner and Burgess (16):

$$T_{\%} = \frac{(24.1)(G)(A)(10^6)}{(W)(MW)(C)} \qquad (31)$$

where $T_{\%}$ is the breakthrough time at a given breakthrough concentration (min), G is the mass of charcoal adsorbent (gm), A is the sorptive capacity at a given percent breakthrough (gm/gm), W is the flow rate (L/min), MW is the molecular weight (gm/mole) and C is the challenge concentration (ppm).

Grubner and Burgess (16) based their predictive equation on the Theory of Statistical Moments (TSM). This theory suggests that the parameters affecting adsorption in a dynamic system are randomly distributed. The change of concentration with time at a given depth of the charcoal bed could be described by a normal probability distribution curve.

APPENDIX B

GASES DETECTED BY THE TGS

FIGARO GAS SENSOR TGS

Several methods of gas detection, based on various chemical and physical principles are now available. A short list includes:

DETECTION TUBE: Based on colour change resulting from a chemical reaction between the gas and the tube contents. This is an accurate quantitative system but each tube can only be used once. It is suitable for spot checking but not for continuous detection.

INFRA RED / SPECTROPHOTOMETRY / GAS CHROMATOGRAPH: These systems provide high continuous accurate detection but costs are high, making them suitable only for specialized industrial applications.

CATALYTIC COMBUSTION: One of the original and most widely used systems based on the temperature change produced by catalytic combustion on a platinum wire sensor. It requires a relatively expensive amplifier and the sensor can be poisoned by silicone and halogen gases. Some technical knowledge is required for operation and maintenance and hence it is recommended for industrial rather than domestic applications.

SEMICONDUCTOR DETECTOR: Introduced by Figaro Engineering Inc. in 1968, the TGS gas sensitive semiconductor sensor is based on N type sintered SnO_2. When combustible or reducing gases are adsorbed on the sensor surface a marked decrease of electrical resistance occurs. Major features of the TGS sensor include high sensitivity (several hundreds ppm of gas easily detected), low cost associated circuitry and the ability to repeatedly detect gas without deterioration. Some of the original sensors produced in 1968 suffered from insufficient mechanical strength and large sensitivity variations, but these problems have been overcome by a continuous programme of research and improvement carried out by Figaro Engineering Inc. When used in accordance with the manufacturer's data a minimum sensor life of 10 years can be expected. By August 1981 more than 13 million TGS sensors were in use worldwide, mainly as domestic gas detectors, making a significant contribution to improved safety.

Main combustible and toxic gases detected by the TGS

Hydrocarbons and Their derivatives: Methane/ Ethane/ Propane/ Butane/ Pentane/ Hexane/ Heptane/ Octane/ Decane/ Petroleum Ether/ Petroleum Benzine/ Gasoline/ Kerosene/ Petroleum Naphtha/ Acetylene/ Ethylene/ Propylene/ Butadiene/ Butylene/ Benzene/ Toluene/ o-Xylene/ m-Xylene/ Ethylene Oxide
Halogenized Hydrocarbons: Methyl Chloride/ Methylene Chloride/ Ethyl Chloride/ Ethylene Chloride/ Ethylidene Chloride/ Trichloro Ethane/ Vinylidene Chloride/ Trichloro Ethylene/ Methyl Bromide/ Vinyl Chloride
Alcohols: Methanol/ Ethanol/ n-Propanol/ iso-Propanol/ n-Butanol/ iso-Butanol
Ethers: Methyl Ether/ Ethyl Ether
Ketones: Acetone/ Methyl Ethyl Ketone
Esters: Methyl Acetate/ Ethyl Acetate/ n-Propyl Acetate/ iso-Propyl Acetate/ n-Butyl Acetate/ iso-Butyl Acetate
Nitrogen Compounds: Nitro Methane/ Mono Methyl Amine/ Dimethylamine/ Trimethyl Amine/ Mono Ethyl Amine/ Diethyl Amine
Inorganic Gases: Ammonia/ Carbon Monoxide/ Hydrogen/ Hydrogen Cyanide

TGS applications

1. Combustible Gas-Leak Alarm
2. Carbon Monoxide Detector
3. Automatic Fan Control
4. Fire Alarm (Detecting combustible gases contained in smoke)
5. Alcohol Detector (Detector for drunken driver)
6. Air Pollution Monitor

TGS features

1. Long life. Sensors in continuous use for 9 years are still functioning normally.
2. High reliability even when exposed to toxic gases.
3. No decrease in sensitivity even when stored for a long period in high humidity atmosphere before use.
4. Detects low concentrations of Natural Gas, Carbon Monoxide and a range of toxic gases.
5. Conforms to vibration and drop test standards.
6. Large resistance change at low gas concentrations enables a reliable low cost detector to be designed.
7. No sensitivity loss even when exposed to high gas concentrations accompanied by reduced oxygen level.

Guidelines for TGS users

1. The sensor is affected to some extent by changes in atmospheric temperature and humidity. For precise work, allowance must be made for these changes.
2. Because the response of the sensor is exponential rather than linear a special circuit must be designed when quantitative measurement is required.
3. The sensor should be powered for several days to ensure it has reached its final stable state i.e. the complete detector should be powered for some days before calibration is carried out.
4. A stabilized sensor requires 1 to 2 minutes recovery time when switched on.

(P.T.O.)

APPENDIX C

CHARCOAL CHARACTERISTICS

CHARCOAL CHARACTERISTICS

Mass of carbon (gm)	49.401
Particle diameter range (mm)	1.40 to 3.35
Bulk density (gm/cm^3)	0.398
Specific bulk volume (cm^3/gm)	2.51
Total void volume (cm^3/gm)	1.62
Solid granule volume (cm^3/gm)	0.89